SWI/SNF ATPase Brahma and Notch signaling collaborate with CBP/p300 to regulate neural stem cell apoptosis in *Drosophila* larval central nervous system.

Punam Bala[1,2], Viswadica Prakki[1] and Rohit Joshi[1,3]

1- Laboratory of Neuroscience and Cell Biology, Centre for DNA Fingerprinting and Diagnostics (CDFD), BRIC-CDFD, Inner Ring Road, Uppal, Hyderabad-500039. India.

2- Graduate studies, Regional Centre for Biotechnology, Faridabad 121001

3- Corresponding author rohit@cdfd.org.in; rj2152@gmail.com

Data Availability Statement: All relevant data are within the manuscript and its Supporting Information files.

Abstract

SWI-SNF ATPase Brahma and Notch signalling are known to interact during development, but how this interaction is executed molecularly is not fully understood. We have investigated the molecular mechanism of Brm-Notch interaction in the context of Hox-dependent neural stem cell (NSC) apoptosis in the developing Central Nervous System (CNS) of *Drosophila*. Our results suggest a multi-tier regulation of NSC apoptosis by Brahma, first by regulating the expression of Drosophila CBP/p300 (Nejire) and the molecular triggers of cell death (Hox, bHLH factor Grainyhead, and Notch signalling pathway). The second mode of regulation is by direct binding of Brahma to the apoptotic enhancer and modulation of the Notch signalling pathway to regulate the *RHG* family of apoptotic genes, *grim and reaper*. Our data support a model where, in response to the apoptotic trigger, Brahma and CSL-Su(H)/Mastermind complex recruit CBP/p300 onto the apoptotic enhancer, thereby increasing the H3K27ac marks on the nucleosomes to facilitate apoptotic gene transcription.

Introduction

Precision of the neural circuitry in the developing central nervous system (CNS) of bilaterian organisms critically relies on generating the right cellular diversity [1]. The generation of this diversity and maintenance of tissue homeostasis in a region-specific manner requires a fine balance of proliferation, differentiation and apoptosis of neural stem cells, neurons and glia [2, 3]. This is directly and indirectly orchestrated in a segment specific manner by Hox family of transcription factors (**TFs**) [4-23]. Programmed cell death (**PCD**-apoptosis) plays a particularly important role in the patterning of the CNS, with neuronal and glial apoptosis being critical for the refinement of the neuronal circuitry [24-26] and neural stem cell apoptosis for bringing about gross patterning changes in the CNS [4, 6, 13, 14, 17, 20-23, 27-29].

During developmental morphogenesis of CNS, the apoptotic triggers range from loss of survival signals, transcriptional induction of pro-apoptotic genes, growth factor signalling, intrinsic transcription factors or a combination of two or more of these events. The transcriptional induction of pro-apoptotic genes is used as a trigger both in vertebrates [30, 31] and invertebrates [8, 10, 20-25]. Segment-specific Hox-dependent neural stem cell (NSCs) apoptosis observed in *Drosophila* CNS, is an example of one such mode of cell death regulation in developing CNS, which is crucial for tissue homeostasis and developmental morphogenesis [4, 6, 10, 13, 14, 17, 21-23]. This mode of NSC (or Neuroblasts –**NBs**) apoptosis happens across the CNS [4, 6, 13, 14, 17, 20-23, 27-29], and has been shown to rely on the resident Hox protein and its cofactor Grainyhead (**Grh**) in larval stages [6, 20, 22, 23, 29]. In the case of abdominal (A3-A7) and terminal (A8-A10) segments of the larval CNS the cell death happens in mid third instar (**mL3**) stage (Fig. 1A), when Grh and the resident Hox factors (expressed in these regions, Abdominal-A and Abdominal-B,

respectively) collaborate with Notch signalling pathway to transcriptionally activate the *RHG* (***reaper, hid and grim***) family of apoptotic genes [32, 33]. This activation happens through a 1 kb enhancer (***F3B3***), deletion of which results in block of NB apoptosis (Fig-1A)[20, 22, 23].

Notch signalling pathway is an evolutionarily conserved, juxtacrine mode of signalling between adjacent cells [34]. The Notch receptor is localised on the membrane of the signal-receiving cell. Upon the activation of Notch by membrane-bound ligands like Delta/Serrate, the Notch intracellular domain (**NICD**) gets cleaved and goes inside the nucleus and binds to the executive transcription factor CSL (or Suppressor of Hairless (**Su(H)** *in Drosophila*) [34]. Following this event, co-repressor binding to Su(H) is replaced by co-activator Mastermind (***mam***), which recruits CBP/p300, a Histone AcetylTransferase (**HAT** encoded by *Nejire-**Nej*** in *Drosophila*) [34, 35], resulting in downstream target gene activation. Expectedly, Notch signalling activation has been shown to bring about CBP/p300 dependent increase in H3K56ac marks and associated chromatin accessibility changes on its target enhancers [35]. In *Drosophila* salivary glands, the enhancer accessibility preceding the signalling activation is shown to be facilitated by SWI-SNF ATPase Brahma (**Brm**), which allows the binding of Su(H) onto the enhancer DNA [36], though this interaction needs to be validated in a developmentally specialised tissue-specific context. Prior studies have also shown a connection between Brm and Notch signalling pathway, with Brm-BAP complex regulating Notch pathway components and its targets [36, 37], similarly, a dominant interaction of Delta and the ATPase dead version of Brm has also been reported [38]. Even though there is evidence of interaction between Brm and Notch signalling during development, the molecular details of how this interaction is effected are not fully understood.

In this work, we investigated Brm and Notch interaction in the context of Hox-dependent NB apoptosis in larval CNS of Drosophila. We find that Brm controls NB apoptosis in terminal segments of the CNS by regulating the expression of Hox (Abdominal-B, **Abd-B**), Grh, and the Notch activity in the NBs. The regulation of the Notch signalling happens at two levels. First, Brm regulates the expression of the members of Notch signalling pathways (like the Notch receptor and its co-activator Mastermind). Second tier of regulation is at the level of the apoptotic enhancer, where Brm interacts with Notch signalling to activate the expression of apoptotic genes *grim* and *reaper*; which is corroborated by an in vitro physical interaction between Su(H) and Brm. The NB apoptosis also required *Drosophila* ortholog of CBP/p300 (Nejire-Nej) at the apoptotic enhancer. Congruent with this, we find that Brm could successfully pull down Su(H), Mam and Nej from larval lysates. Collectively, our results support a model where Brm regulates the enhancer accessibility and activation of apoptotic genes, indirectly by modulating the expression of Hox, Grh, CBP/p300 and the members of the Notch signalling pathway, and directly by regulating the recruitment of Su(H)/CBP signalling complex onto the apoptotic enhancer.

Results

ATPase activity of Brahma is required for NB apoptosis in larval CNS.

The NBs in abdominal (30 in A3-A7) and terminal (20 in A8-A10) segment of the larval ventral nerve cord (**VNC**) start dying in second instar stage and are completely eliminated from VNC by late L3 stage (**LL3**) [22, 23]. In the terminal segments, NBs are classified based on the expression of the *doublesex* gene (*dsx*) [22]. In female CNS, four Dsx-positive NBs undergo sex-specific apoptosis (which is

independent of Grh and Notch) in mid L2 stage of development [21](Fig. 1A). Their counterparts in male CNS continue dividing till pupal stages. The remaining 16 Dsx-negative NBs die in mL3 stage [22] and are studied and analysed here.

We identified SWI-SNF ATPase Brahma (*brm*) in an RNA interference (RNAi) screen for genes regulating NB apoptosis in abdominal and terminal segments of larval ventral nerve cord. We tested five RNAi lines targeted against different regions of the Brm cDNA and observed that three of these lines (detailed in methods) showed a block of NB apoptosis in larval VNC. Owing to better consistency of the expression of the previously characterised *enhancer-lacZ* line (*F3B3-lacZ*), and the fact that the *brm* knockdown was unable to block the apoptosis of Dsx-positive NBs in the female CNS, we focused our experiments and analysis on Dsx-negative NBs found in the A8-A10 segments of the female larval CNS. These cells were identified by costaining with NB marker Deadpan (Dpn) and resident Hox factor Abd-B, and none of these NBs survive by the late L3 stage in female CNS [21, 22].

We observed that Brm-knockdown (using NB expressing *inscGAL4*) could block the death of Dsx-negative NBs (Fig. 1B-1C and 1F). All three lines blocked apoptosis when the knockdown was induced from the embryonic stages. We also observed a block of NB apoptosis in the case of Moira and Snr1 (two RNAi lines each), which are components of the Brm-associated core complex (Fig. S1C-S1F). Thereafter, we did a rescue experiment to establish the specificity of the phenotype and conservation of the function of the *brm* gene across species. We could partially rescue the block of NB apoptosis by overexpression of the *Drosophila brm* gene, as well as with its human ortholog (hSMARCA2) (Fig 1F). To further confirm the phenotype, we tested a weak heteroallelic mutant combination for the hypomorphic alleles of *brm* gene ($brm^{d00415/l21}$), which survived till late third instar larval stage

(LL3) of development, and we could observe a block of NB apoptosis in this case as well (Fig. 1J and 1M). Next, we tested the role of BAP and PBAP complex in NB apoptosis. Here we observed that knockdown for Osa, which is a BAP complex specific subunit, blocked the NB apoptosis (Fig. S1J-S1K); while the knockdown for PBAP complex-specific subunits (like SAYP, BAP170, and Polybromo) did not (Fig. S1L-S1Q).

Thereafter, we tested the contribution of Brm's chromatin remodelling activity in NB apoptosis. The remodelling activity of Brm relies on the ATPase domain, and mutating lysine-804 to an arginine (K804R) is known to abrogate it [39-41]. We observed that overexpression of the ATPase domain dead version of the Brm (Brm-K804R) also blocked NB apoptosis in A8-A10 segments (Fig. 1E and 1F), comparable to what was seen in the case of *brm-RNAi*. To conclusively establish the role of K804 in NB apoptosis, CRISPR-Cas9 was used to mutate lysine 804 to arginine in *brm* (brm^{K804R}). A weak heteroallelic mutant combination of the CRISPR allele and hypomorphic allele ($brm^{d00415/K804R}$) survived till the LL3 stage of development and also showed a block of NB apoptosis (Fig. 1L and 1M).

These results established that the Brm-associated BAP complex is important in executing Hox-dependent NB apoptosis and relies on its ATPase activity for this function. The rescue of the block of NB apoptosis by the human ortholog hSMARCA2 suggests a conservation of gene function across species.

Brm regulates NB apoptosis by regulating Hox, Grh and Notch signalling pathways.

Next, we checked the levels of Grh, Hox and Notch activity, which function as trigger for A8-A10 NB apoptosis. This was done by comparing Hox and Grh expression levels and Notch activity in these cells in controls and in case of *brm* knockdown. The controls in this case were the larvae, where the NB apoptosis was blocked by expression of the cell death blocker p35. The Notch activity was monitored using E(spl)mγ-GFP, which shows a strong expression and is known to be responsive to Notch signalling in NBs [42]. We observed that Brm-knockdown resulted in a significant reduction in the levels of AbdB (Fig. 2B'), Grh (Fig. 2E') and a complete loss of E(spl)mγ-GFP (Fig. 2H') in the NBs in A8-A10 segments.

Thereafter, we tested if *brm* knockdown affected Notch signalling by regulating the expression levels of the members of the Notch signalling pathway. We checked the levels of the Notch receptor, N; the executive TF of Notch pathway, Su(H); ligand Delta, Dl; and co-activator, Mastermind (Mam). We observed that while levels of the Su(H) and Dl were unaffected (Fig. 2O and 2Q), the levels of N (Fig. 2J and 2N), and the co-activator Mam (Fig. 2L and 2P) were found to be significantly reduced in the NBs of A8-A10 segments.

These results collectively suggested that Brm knockdown blocks A8-A10 NB apoptosis by regulating Hox, Grh and Notch activity. The impact on the Notch activity seems to be through regulation of the levels of N, and Mam.

Notch and Brm interact to regulate NB apoptosis.

In the salivary gland Brm facilitates Su(H) binding on Notch target enhancers [36]. Considering this, we decided to check the interaction between Brm and Notch. We could observe a weak but robust dominant interaction between the heterozygous

null alleles of *brm* and *Notch* ($N^{55e11/+}$; $brm^{2/+}$), which showed a block of apoptosis of NBs in A8-A10 segments (Fig. 3D and 3E). This was further substantiated by the double knockdown of Su(H) and Brm, wherein we observed a cumulative increase in the number of surviving NBs in A8-A10 segments (Fig 3F), suggesting that the two are functioning together. The single knockdown of Su(H) also blocked NB apoptosis and compromised Notch signalling (Fig. S2).

A 1Kb *enhancer* (*F3B3*) (Fig. 3G), which starts expressing in the NBs in the mid-second instar stage, is suggested to be responsible for the activation of apoptotic genes *grim and reaper* and consequent death of A8-A10 NBs [22]. Since deletion of 717 bps of this enhancer blocks the NBs apoptosis (*Δ717/Δ717*) [22], we checked if Brm bound to this enhancer. For this, we used the Targeted DamID (TaDa) technique [43] to check for Brm binding onto the apoptotic enhancer in NBs of larval CNS. TaDa allows probing tissue-specific in vivo binding status of chromatin/DNA binding proteins. To monitor the Brm binding onto the 1 Kb apoptotic enhancer, we divided it into five fragments of approximately 200 bps and designed primers for these amplicons to assay the enrichment of Brm bound fragments using RealTime (RT) PCR (Fig. 3G). Using the TaDa-RT PCR, we found that Dam-Brm fusion showed 2-fold enrichment compared to the Dam-only control for all five fragments (Fig. 3I), suggesting that Brm bound to the 1 Kb apoptotic enhancer in the NBs. We could also observe the Brm binding onto the intergenic region between mβ and mα genes and mβ-tr (mβ-transcribed region) of the Enhancer of Split [E(spl)] complex (Fig 3H and 3I). E(spl) complex is a known target for Notch signalling, and the intergenic region between E(spl)-mβ and mα is known to be bound by Brm [36], which therefore acted as positive controls for us. Subsequently, we reanalysed an already published Targeted DamID-seq data [44] for NBs in the early L3 stage of

development and found that Brm bound to the 1kb enhancer (*F3B3*) in NBs (Fig. S3), reaffirming our results. We also found significant Brm binding on apoptotic genes, *grim* and *reaper*, in addition to *N* and *Mam* (Fig. S3).

Considering our genetic data (dominant genetic and RNAi interactions) as well as previously published results, where Brm binding is required for Su(H) to bind to DNA [36], we expected that Brm and Su(H) may physically interact with each other. Therefore, we checked this using an in vitro pulldown experiment wherein different regions of Brm (Fig. 3J) were tested for their interaction with Su(H). Here we found that Brm and Su(H) interact with each other through HSA and BRK domains of Brm (Fig. 3K-3M), which are important for Brm's interaction with chromatin and act as a primary binding platform for actin and ARP (actin related proteins) to regulate chromatin remodelling function [45-47].

Collectively, these results show that Brm and Notch show a dominant genetic interaction, with Brm binding to the enhancer being required for NB apoptosis. We also find that Brm physically interacts with Su(H) through its HSA and BRK domains.

Brm regulates *grim* and *reaper* genes through the *F3B3* enhancer.

Next, we functionally tested whether the *brm* knockdown-mediated block of NB apoptosis happened through its impact on the *F3B3* enhancer. For this, we checked the expression of the *F3B3-lacZ* in the case of the *brm* knockdown as well as in the case of overexpression of the catalytically dead version of Brm (Brm-K804R). The controls in this case were the larvae, where NB apoptosis in the CNS was blocked by expression of the cell death blocker p35. Here, we observed a significant decrease in the percentage of cells expressing *F3B3-lacZ* in *brm*

knockdown and overexpression of Brm-K804R compared to NBs in p35 expressing control CNS (Fig. 4A). We also tested knockdown for Notch and Mam for their impact on *F3B3-lacZ* line expression in NBs. The control VNCs typically have 70% of the A8-A10 NBs expressing *F3B3-lacZ* in the early L3 stage; this number was reduced to 26% in the case of *brm*-knockdown, 32% in case of overexpression of BrmK804R and 17% and 8% in the case of Notch and Mam knockdown (Fig. 4A). We also observed that knockdown for Mam resulted in block of NB apoptosis and reduction in Notch activity (Fig. S2). These results suggest that the block of apoptosis that is seen in the case of *brm, Notch* and *Mam* knockdowns, and in case of the overexpression of catalytically dead Brm are mediated through their impact on the *F3B3* enhancer. Next, we checked if the homozygous deletion of the apoptotic enhancer (*Δ717/Δ717*) resulted in downregulation of the *grim* and *reaper* transcripts in the CNS and observed approximately a 50% decrease in the transcript levels (Fig. 4B).

Considering the reduction in the number of *F3B3-positive* NBs in Brm knockdown, we decided to check the impact of the Notch-Off and Brm-Off conditions individually and collectively on the *grim and reaper* transcript levels. For this, we did a knockdown of Notch ligand Delta (Notch-Off condition), a knockdown of the *brm* gene (Brm-Off), and a combined knockdown of the two. In the case of *reaper* gene, we observed only a modest decrease in transcript levels in case of Notch-Off and Brm-Off. However, in the case of *grim* gene, we observed a 50% and 60% decrease in the transcript levels in the case of Notch-Off and Brm-Off conditions, respectively (Fig. 4C). The reduction in Dl and Brm transcripts was confirmed in the case of single (Notch-Off, Brm-Off) and collective knockdowns (Fig. 4D and 4E).

In case of double knockdown, we observed only a 50% decrease for *grim*, similar to what is seen in the case of Notch-Off condition, which suggested that Notch signalling functions downstream of the Brm to regulate apoptotic genes. To probe the hierarchical relation between Notch and Brm, we also assayed the number of surviving A8-A10 NBs. To this end, we overexpressed Brm in the case of Notch, Su(H) and Mam knockdowns (which blocked NB apoptosis to varying extents). In all these cases, we observed that overexpression of Brm did not result in any change in the block of NB apoptosis seen in A8-A10 segments, thereby further establishing that Brm is genetically upstream to Notch signalling pathway.

Considering these results and Targeted DamID data, we favour that Brm regulates apoptosis by regulating the expression of *grim* and *reaper* genes, through its direct binding on the *F3B3* enhancer. Collectively, our results suggest that Brm functions upstream of the Notch signalling pathway, but also collaborates with it at the level of the *F3B3* enhancer.

Drosophila CBP/p300 recruitment onto the apoptotic enhancer is important for Notch activity and apoptosis.

A rapid and large-scale change in the H3K56ac is reported in case of Su(H) bound Notch target enhancers upon Notch signalling activation. This is dependent on CBP/p300 (encoded by the *nejire* (*nej*) gene in *Drosophila*) and leads to increased transcription following Notch signalling activation [35]. Therefore, we tested the role of Nej in A8-A10 NB apoptosis. As the H3K56ac antibody did not show a good staining in NBs of the CNS, we used the H3K27ac antibody to monitor the acetylation status of nucleosomes and to assay the role of the Nej.

We observed that Nej knockdown resulted in the block of NB apoptosis in A8-A10 segments (Fig. 5B and 5L). Expectedly, we also observed that levels of H3K27ac in the surviving A8-A10 NBs were reduced in the case of the Nej knockdown (Fig. 5D' and 5M). Considering that Nej mediated histone acetylation is important for increased transcription of the Notch targets, we checked the E(spl)mγ-GFP expression in these NBs and observed a significant reduction in its levels in case of Nej knockdown (Fig. 5F' and 5N). Next, we checked the impact of Nej knockdown on the apoptotic enhancer. We observed a significant decrease in the percentage of cells expressing *F3B3-lacZ* compared to controls (Fig. 5G), suggesting that the block of apoptosis in Nej knockdown was mediated through its impact on the apoptotic enhancer. Thereafter, we checked if Brm knockdown affected Nej levels in the NBs. Here, we observed a 40% reduction in the levels of Nej (Fig. 5O) and a decrease in H3K27ac marks on the nucleosomes in the surviving A8-A10 NBs (Fig. 5J' and 5M). These results suggested that Brm is upstream of Nej, which was further supported by the fact that its overexpression did not rescue the block of NB apoptosis and the reduction in the levels of H3K27ac seen in the case of Nej knockdown (Fig. 5K', 5L and 5M). Congruent to this, we could observe significant Brm binding on the *nej* gene (Fig S3) in published TaDa data for Brm [44].

Since our previous results supported the idea that one of the ways Brm mediates the block of NB apoptosis is by binding to the *F3B3* enhancer, where it may interact with Su(H). We speculated that upon signalling activation, NICD binds to the signalling complex (Su(H) and Mam) and recruits Nej to increase acetylation at the *F3B3* enhancer. If this were to be the case, we expected that all these factors might function as a complex in vivo. Congruent with this, Brm could pull down Su(H), Mam and Nej from larval lysates (Fig. 5P).

Our results suggest that Nej-mediated H3K27 acetylation at the Notch-sensitive *F3B3* enhancer contributes to NB apoptosis. The pulldown from the whole larval lysates confirms that components of the Notch pathway, Brm, and Nej exist in a complex, supporting the idea that Brm interacts with the Notch-Nej complex to facilitate NB apoptosis.

Discussion

Brm and Notch signalling have been shown to interact during development [36-38], but how this interaction is executed molecularly is not fully understood. The CBP-dependent increase in H3K56ac/H3K27ac and elevated transcription at the Notch targets upon signalling activation has been shown in *Drosophila* and vertebrate cell culture [35]. Similarly, the role of the Brm in mediating the binding of Su(H) onto the DNA to facilitate Notch-dependent transcription has also been established [36]; however, the in vivo validation of this interaction in a physiological context has been missing. We have investigated the molecular mechanism of this interaction in the context of Hox-dependent NB apoptosis in larval CNS. Our results suggest a multi-tier regulation of NB apoptosis by SWI-SNF ATPase Brahma in the larval CNS. The first tier of regulation is in controlling the expression of the *Drosophila* homolog of CBP/p300 (Nej-a HAT) and the molecules directly involved in the cell death (Hox, Grh, and members of the Notch signalling pathway). The second tier of regulation is by direct binding and modulation of the chromatin accessibility at the apoptotic enhancer. This facilitates the binding of Su(H) onto the enhancer (as suggested earlier) [22], and keeps it ready to respond to the apoptotic trigger (which is an increase in the levels of Grh and Notch activity). Our data support a model

where, in response to the apoptotic trigger, Brm and Su(H)/Mam complex recruit CBP/p300 (Nej) onto the apoptotic enhancer, increase the H3K27ac marks on the nucleosomes, and facilitate *grim* and *reaper* transcription. The role of Brm in regulating the H3K27ac through its direct interaction with CBP has been reported earlier as well [48], though the Brm-CBP-mediated modulation of Notch signalling in the context of NB apoptosis is novel.

The Brm-associated BAP complex is conventionally known to be involved in activating gene transcription. However, a recent study showed that the BAP complex and its subunit Osa can also cause gene repression. This study showed that Osa was bound to the components and targets of the Notch signalling pathway to constrain their expression [37]. Expectedly, the loss of Osa resulted in activation of Notch ligand Delta in the wing disc. Considering the role of the Brm as a chromatin remodeller, we expected it to regulate NB cell death by positively regulating the expression of the *RHG* family of apoptotic genes. Congruent with this, the knockdown of Brm, Moira and Snr1, which are core components of the Brm complex and Osa, a BAP complex-specific subunit, blocked NB apoptosis (Fig. S1). On similar lines, the knockdown of PBAP complex members like SAYP, BAP170, and Polybromo did not block of NB apoptosis (Fig. S1), thereby reiterating the role of BAP complex in gene activation in this context.

The first tier of regulation mentioned above established one way of interaction between Brm and Notch signalling pathway. Other supporting evidence being the dominant genetic interaction between mutants of *Notch* and *brm* heterozygotes, and the double knockdown of Brm and Su(H), both of which resulted in the block of NB apoptosis. This is expected considering a past report where the Notch ligand Dl showed a dominant genetic interaction with ATPase dead Brm [38]. However,

evidence also support the idea that this interaction also happens at the level of the apoptotic enhancer. First being that both Su(H) [22] and Brm bind to the apoptotic enhancer (TaDa data), and their respective knockdowns (this study and [22]) reduced the expression of *F3B3-lacZ* in the NBs of the CNS. On these lines, we observed that individual knockdown of Brm did not affect Cut (a target of Notch signalling) expression in the NBs, but the double knockdown of Brm and Su(H) reduced the expression of Cut to an extent greater than what is seen for Su(H) knockdown alone (Fig. S5), further suggesting for a collective role of the two "on the DNA" rather than "off the DNA". Other supporting evidence is the in vivo pulldown from the larval lysates, which shows that Brm, Su(H), Mam, and CBP/Nej may exist as a complex in a cell, which is likely to be on the DNA, considering that all of them are DNA/chromatin binding proteins. The in vitro pulldown showing that Brm and Su(H) physically interact with each other through Brm's highly conserved HSA and BRK domains, lead us to further favour the idea that this interaction may be happening on the apoptotic enhancer, since these domains act as a binding platform for actin-related proteins (ARPs) and help Brm to perform its remodelling function [45-47]. Lastly, whether disrupting this interaction can actually impact the in vivo functionality of the complex and block Hox-dependent NB apoptosis needs to be tested.

Figure legends

Figure 1*:* ATPase activity of Brm is required for A8-A10 NB apoptosis

(A) Schematic of larval CNS showing Hox-dependent NB apoptosis in abdominal (A3-A7) and terminal (A8-A10) segments. In Abd-B expressing terminal (A8-A10)

segments, NBs are categorized based on the expression of *doublesex* (*dsx*). In female CNS, Dsx-positive NBs use Abd-B and Dsx^F (female-specific isoform) to undergo apoptosis, while in males, these NBs continue dividing till late pupal stages. Dsx-negative NBs (hereon referred to as A8-A10 NBs) use Hox (Abd-B), Grh and Notch signalling to transcriptionally activate RHG family of apoptotic genes (*grim* and *reaper*) through a 1 kb enhancer (*F3B3*) and undergo apoptosis in mid L3 stage. **(B-E)** Shows terminal segments of late L3 stage CNS with no surviving (A8-A10) NBs in case of controls (*inscGAL4>GFP*) (B, D) (0±0 NBs, $n = 8$ VNCs, N = *2*) and ectopic NBs in *brm-RNAi* (10.83±0.13 NBs, $n = 12$ VNCs, N = 3) and over-expression of HA-tagged Brm-K804R (10.44±0.88 NBs, $n = 9$ VNCs, $N = 3$). This establishes that *brm* knockdown blocks NB apoptosis, and ATPase activity of Brm is required for this apoptosis. **(F)** Graph showing the number of surviving A8-A10 NBs in the case of CNS of controls, *brm-RNAi,* and *brm-K804R*. Graph also shows the number of surviving NBs when the *brm-RNAi* phenotype was rescued using overexpression of Drosophila Brm (*HA-brm*; 4.00±0.29 NBs, $n = 10$ VNCs, $N = 4$), and the human ortholog of *brm (HA-hSMARCA2;* 3.07±0.49 NBs, $n = 14$ VNCs, $N = 4$) (Bars 5, and 7), establishing cross-phylum conservation of the Brm function. **(G-L)** Shows that no NBs survive in CNS of controls (*Canton S*) and heterozygotes for *brm* alleles ($brm^{d00415}/+$ and $brm^{l21}/+$; $brm^{K804R}/+$; 0±0 NBs, $n = 7$ VNCs, $N = 2$), but NBs apoptosis is blocked in hetero-allelic combinations of *brm* ($brm^{d00415/l21}$; 6.18±2.35 NBs, $n = 11$ VNCs, $N = 4$; $brm^{d00415/K804R}$; 4.00±1.22 NBs, n =5 VNCs, $N = 2$). **(M)** Graph showing the number of surviving A8-A10 NBs in heterozygous controls and heteroallelic *brm* mutant combinations. Yellow arrowheads indicate the ectopic NBs. Scale bars are 10 µm. Graph shows mean±SD. Significance is from a two-tailed Students' unpaired *t-test*.

Figure 2: Brm controls A8-A10 NB apoptosis by regulating expression of Hox, Grh, NICD and Mam.

(A-B, D-E, G-H, I-J, K-L) Show levels of Hox (Abd-B; 2.71±0.92; 93 NBs, *n*=9 VNCs *N* = 3) (A), Grh (67.05±31.57; 79 NBs, *n*=7 VNCs *N* = 3) (D), E(spl)-mγ-GFP (35.76±23.78; 78 NBs, *n*=10 VNCs *N* = 5) (G), NICD (12.63±4.52; 99 NBs, *n*=8 VNCs N = 3) and Mam (25.28±17.69; 78 NBs, *n*=7 VNCs *N* = 3) in control CNS, where NB apoptosis is blocked by expression of p35. Compared to these controls the knockdown of *brm* (*brm-RNAi*) leads to a significant reduction in the levels of Hox (1.84±0.73; 91 NBs, *n* = 14 VNCs, *N* = 3) (B), Grh (23.22±13.15; 73 NBs, *n*=10 VNCs, *N* = 3) (E), and E(spl)-mγ-GFP (13.52±14.46; 97 NBs, *n*=10 VNCs *N* = 5) (H), NICD (10.18±5.72; 95 NBs, n=14 VNCs, N= 3) (J) and Mam (14.29±6.80; 94 NBs, *n*=13 VNCs *N* = 3) (L). Graphs comparing the levels of Hox **(C)**, Grh **(F)**, E(spl)-mγ-GFP **(M)**, NICD **(N)**, Su(H) **(O)** and Mam **(P)**, Delta **(Q)** in A8-A10 NBs in p35 expressing control CNS and those with Brm knockdown (*brm-RNAi*). Yellow arrowheads indicate the ectopic NBs. Scale bars are 10 µm. Graph shows mean±SD. Significance is from a two-tailed Students' unpaired *t-test*.

Figure 3: Brm binds to the *F3B3* apoptotic enhancer and dominantly interacts with the Notch signalling pathway.

(A-D) Shows dominant interaction of $N^{[55e11]}$ and brm^2. The terminal segments of the late L3 stage CNS show no surviving NBs in the case of control (*Canton-S;* 0±0 NBs, *n* = 8 VNCs, *N* = 2), *brm* heterozygotes ($brm^2/+$**;** 0±0 NBs, *n* = 8 VNCs, *N* = 2), *Notch* heterozygotes ($N^{[55e11]}/+$**;** 0±0 NBs, *n* = 7 VNCs, *N* = 3), but the double heterozygotes for *Notch* and *brm* ($N^{[55e11]}/+$**;** $brm^2/+$) shows ectopic NBs (4.50±0.75

NBs, $n = 8$ VNCs, $N = 4$). **(E)** Graph showing number of surviving NBs in A8-A10 segments in control (*inscGAL4>GFP*) and test (*brm*^{2}, and *N*$^{[55e11]}$ heterozygotes and double heterozygotes *N*$^{[55e11]}$*/+;brm*^{2}*/+*) in late L3 stage CNS. **(F)** Graph showing number of surviving NBs in A8-A10 segments in controls (*Canton S*; 0±0 NBs, $n = 8$ VNCs, $N = 3$) and *brm-RNAi* (10.83±0.13 NBs, $n = 12$ VNCs, $N = 3$), *Su(H)-RNAi* (11.63±0.91 NBs, $n = 9$ VNCs, $N = 3$) and double knockdown (*brm-RNAi* and *Su(H)-RNAi;* 18.63±3.11 NBs, $n = 8$ VNCs, $N = 4$) in late L3 stage CNS. **(G)** Schematic showing the genomic location of *NBRR* region, *grim* and *reaper* genes on chromosome 3L. Green line shows the *F3B3* enhancer and red lines shows the extent of deletion. The 1 kb region is subdivided into 5 fragments of approximately ~220 bp for *brm* binding study. **(H)** Schematic shows the representation of the genomic locus of *E(spl)-C* genes on Chr 3R. The regions indicated by arrow are the regions used as positive controls for Brm binding by an earlier study (Pillidge and Bray, 2019)**. (I)** Targeted DamID experiments show that Brm binds to the *F3B3* enhancer in the NBs. Fold enrichment graph of different fragments of *F3B3* for Dam-Brm compared to Dam-only (control) shows Brm binding onto the *F3B3* enhancer. *mβ-tr*, *mβ-enh* and *mβ-mα-igr* are used as the positive controls for the binding on *E(spl-C).* **(J)** Schematic showing domains of Brm protein (Brm-FL), and domains retained in deletion fragments of Brm, which are used for the in vitro pull-down. **(K-M)** Shows that Brm physically interacts with Su(H). GST tagged Su(H) could pull down BrmF2 **(L)**, but not BrmF1 **(K)** and BrmF3 **(M)**. Coomassie blue gel depicts the loading of GST-tagged Su(H). Yellow arrowheads indicate the ectopic NBs. Scale bars are 10 µm. Graph shows mean±SD. Significance is from a two-tailed Students' unpaired *t-test*.

Figure 4: Brm regulates transcription of *grim* and *reaper* through the *F3B3* enhancer.

(A) Graph comparing the percentage of LacZ-positive and LacZ-negative NBs in A8-A10 segments of in late L3 stage CNS; p35 expressing control larvae are compared with *brm-RNAi, brm-K804R, Notch-RNAi* and *Mam-RNAi.* **(B)** Graph shows that compared controls (*Canton S*) the transcript levels of *grim* and *rpr* are reduced in homozygous deletion for apoptotic enhancer *F3B3* (*Δ717/Δ717).* The result suggests that *brm* regulate transcripts of *grim* and *reaper* through *F3B3* apoptotic enhancer. **(C)** Graph compares the transcript levels of *grim* and *reaper* in *Dl-RNAi* (Notch-OFF), *brm-RNAi* (Brm-OFF) and collectively in double knockdown for the two (*Notch*-OFF+*Brm*-OFF). The transcript levels for *grim* are reduced in single knockdown; the extent of reduction in double knockdown is similar to Notch-OFF, suggesting that Notch is downstream of Brm. **(D-E)** Shows that the transcript levels of *Dl* and *brm* go down in the individual and double knockdowns. **(F)** Graphs show the number of surviving NBs in A8-A10 segments for the controls (0±0 NBs, $n = 8$ VNCs, $N = 3$), *brm* overexpression (0±0 NBs, $n = 10$ VNCs, $N = 3$), *Notch-RNAi* (20.50±3.70 NBs, $n = 8$ VNCs, $N = 3$), *Su(H)-RNAi* (5.70±1.82 NBs, $n = 10$ VNCs, $N = 3$), *mam-RNAi* (22.90±1.28 NBs, $n = 10$ VNCs, $N = 4$) and the rescue experiments where *brm* is over-expressed in *Notch-RNAi* (20.00±1.52 NBs, $n = 13$ VNCs, $N = 3$), *Su(H)-RNAi* (4.41±0.79 NBs, $n = 12$ VNCs, $N = 3$) and *mam-RNAi* (20.36±4.43 NBs, $n = 11$ VNCs, $N = 4$) backgrounds. These experiments establish that *Notch* is downstream of *brm,* since *brm* overexpression fails to rescue the knockdowns of *Notch, Su(H) and Mam.* Graph indicating mean±SD. The transcript levels in panels **B**, **C**, **D** and **E** are normalised to GAPDH expression levels in control and tests. Significance is from two-tailed Students' unpaired t-test.

Figure 5: *Drosophila* ortholog of histone acetyl transferase CBP/p300 (Nej) is required for NB apoptosis and is regulated by *brm*.

(A-B) Compared to controls (*inscGAL4>GFP*; 0±0 NBs, $n = 9$ VNCs, $N = 3$) knockdown of *Drosophila* CBP/p300 (*nej-RNAi*; 5.00±1.35 NBs, $n = 13$ VNCs, $N = 3$) blocks A8-A10 NB apoptosis. **(E-F)** The knockdown of Nej (*nej-RNAi*) leads to a significant reduction in the levels of E(spl)-mγ-GFP (20.41±10.58, 81 NBs, n=9 VNCs, $N = 3$) (F) in A8-A10 NBs compared p35 expressing control NBs (48.17±26.34, 131 NBs, n=7 VNCs, $N = 2$) (E) (blocked for apoptosis); indicating that Notch activity is abrogated in Nej knockdown. **(H-I)** The knockdown of *brm* (*brm-RNAi*) leads to a significant reduction in the levels of Nej (30.07±22.68, 76 NBs, n=10 VNCs $N = 2$) (I) in A8-A10 NBs compared to p35 expressing control NBs (59.77±26.90, 78 NBs, n=7 VNCs $N = 2$) (H), indicating that Nej levels are affected in the case of *brm* knockdown. **(C-D, J-K)** Shows a significant reduction in the levels of H3K27ac in the case of the knockdown of Nej (*nej-RNAi;* 3.3±2.37, 112 NBs, n=11 VNCs, $N = 3$) (D) and *brm* (*brm-RNAi;* 26.16±18.78, 97 NBs, n=17 VNCs, $N = 4$) (J) in A8-A10 NBs compared to p35 expressing control (47.72±29.46, 93 NBs, n=6 VNCs, $N = 2$) (C). The reduction in H3K27ac levels seen in the case of Nej knockdown is not rescued by overexpression of *brm* (2.80±1.36, 91 NBs, n=9 VNCs $N = 2$) in these cells, indicating that Nej is downstream of Brm. **(G)** Graph comparing the percentage of LacZ-positive and LacZ-negative NBs in A8-A10 segments of in late L3 stage CNS; p35 expressing control larvae are compared with *nej-RNAi.* The result suggests that *nej* impacts NB apoptosis through *F3B3* enhancer. **(L)** Graph comparing the number of surviving A8-A10 NBs in controls (*inscGAL4>GFP*; 0±0 NBs, $n = 8$ VNCs, $N = 2$), *brm* overexpression (0±0 NBs, $n = 10$ VNCs, $N = 3$), *nej* knockdown (*nej-RNAi*; 5.00±1.35 NBs, $n = 13$

VNCs, $N = 3$) and *brm* overexpression in the background of *nej* knockdown (6.30±2.11 NBs, $n = 10$ VNCs, $N = 5$). **(M)** Shows the graph comparing the levels of *H3K27ac* level in A8-A10 NBs expressing *p35, nej-RNAi, brm-RNAi and brm* overexpression in *nej-RNAi*. The data in (L) and (M) show that Brm overexpression could not rescue Nej, establishing that Nej functions downstream of Brm. **(N)** Shows that Nej knockdown reduces E(spl)-mγ-GFP expression levels in A8-A10 NBs compared to p35 expressing control NBs (blocked for apoptosis). **(O)** Shows that Brm knockdown results in downregulation of Nej levels in A8-A10 NBs compared to p35 expressing control NBs (blocked for apoptosis). **(P)** Western blot showing that Brm could pull down Su(H), Mam and Nej from larval lysates. IgG in the first lane is used as a negative control, which does not interact with components pulled down in the experiment. Yellow arrowheads indicate the ectopic NBs. Scale bars are 10 µm. Graph shows mean±SD. Significance is from a two-tailed Students' unpaired *t-test*.

Figure 6:

(A) Schematic suggesting that Brm regulates the levels of Hox *(*Abd-B*)*, Grh*,* and components of Notch signalling pathway (NICD, Mam) and Histone Acetyl Transferase CBP/p300/Nej. **(B)** Prior to activation of Notch signalling, Brm opens the chromatin and facilitates the binding of Su(H) onto DNA. Upon activation of Notch signalling by NICD binding to Su(H), the corepressor is removed and coactivator Mastermind is recruited, which then recruits histone acetyl transferase CBP/p300/Nej to the Notch signalling complex, increasing the H3K27ac, resulting in further opening of the chromatin and transcriptional activation of *grim* and *reaper.*

Supplementary Figures

Fig. S1: BAP Complex is responsible for NB apoptosis

(A) Schematic showing the components of BAP and PBAP complexes. The core subunits are shown in 3 colors: pink (Moira, Snr1), green (Bap111, Bap60, Bap55 and Actin) and red (Brm). The complex-specific subunits are blue (Osa for BAP; Polybromo, BAP170, Sayp for PBAP). (B-I) Knockdown of Snr1 and Moira results in a block of A8-A10 NB apoptosis. The CNS from controls (*inscGAL4>GFP*; 0±0 NBs, $n = 8$ VNCs, $N = 2$) (B) show no surviving NBs while knockdown for Moira (*Moira-RNAi-1 and 2;* 5.91±1.67 NBs, $n = 18$ VNCs, $N = 6$; 7.57±1.83 NBs, $n = 9$ VNCs, $N = 3$) (C, D) and Snr 1 (*Snr1-RNAi-1 and 2;* 8.42±2.63 NBs, $n = 15$ VNCs, $N = 4$; 5.50±3.39 NBs, $n = 7$ VNCs, $N = 4$) (E, F) blocks NB apoptosis in late L3 CNS. Knockdown for Bap111 (G-H) and Bap55 (I) did not show any surviving NBs. **(J-K*)*** Compared to controls (*inscGAL4>GFP*; 0±0 NBs, $n = 8$ VNCs, $N = 2$) (B), knockdown of BAP complex specific subunit Osa (*Osa-RNAi-1 and 2;* 6.53±1.71 NBs, $n = 15$ VNCs, $N = 3$, 5.66±2.29 NBs, $n = 10$ VNCs, $N = 4$) (J-K) results in a block of A8-A10 NB apoptosis. In contrast, the knockdown of PBAP-specific subunits Sayp*,* Polybromo and Bap170 (L-Q) does not block NB apoptosis. (R-T) Graph showing the surviving A8-A10 NBs in case of the knockdown for core (R) and BAP (S) and PBAP (T) specific subunits of the complex. Yellow arrowheads indicate the ectopic NBs. Scale bars are 10 µm. Graph shows mean±SD. Significance is from a two-tailed Students' unpaired *t-test*.

Fig. S2: Knockdown of *Notch, Su(H) and Mam*

(A-D) Knockdown of Notch, Su(H) and Mam results in a block of A8-A10 NB apoptosis. The CNS from controls (*inscGAL4>GFP*; 0±0 NBs, $n = 8$ VNCs, $N = 2$) (A) show no

surviving NBs while knockdown for Notch (*Notch-RNAi-1* 21.50±5.01 NBs, $n = 8$ VNCs, $N = 3$) (B), Su(H) (*Su(H)-RNAi;* 11.63±0.30 NBs, $n = 8$ VNCs, $N = 3$) (C), and Mam (*mam-RNAi*; 24.10±0.57 NBs, $n = 10$ VNCs, $N = 3$) (D) blocks NB apoptosis in late L3 CNS. (F-H) Show levels of E(spl)-mγ-GFP in control NBs blocked for apoptosis by expression of p35 (48.17±26.34, 131 NBs, n=7 VNCs $N = 3$) (A). The E(spl)-mγ-GFP expression is significantly reduced in A8-A10 NBs upon the knockdown of Su(H) (*Su(H)-RNAi*) (C) and Mam (*mam-RNAi*) (D) in the late L3 stage. (E) Graph showing the number of surviving A8-A10 NBs in late L3 stage CNS in *Control (inscGAL4>GFP), Notch-RNAi, Su(H)-RNAi* and *Mam-RNAi*. (I) Graph comparing the levels of E(spl)-mγ-GFP in A8-A10 NBs of controls, Su(H) and Mam knockdown. Yellow arrowheads indicate the ectopic NBs. Scale bars are 10 µm. Graph shows mean±SD. Significance is from a two-tailed Students' unpaired *t-test*.

Fig. S3: Targeted Dam ID shows that Brm binds to *grim, reaper, F3B3, Notch, mam, nej* and *Su(H)*

Shows binding profile of Brm on *grim (A), reaper (A)*, *F3B3* apoptotic enhancer (A), *Notch* (B), *mam* (C), and *nej* (D) in NBs at the mid L3 stage in larval CNS as identified by Targeted Dam ID. The binding profiles suggest that Brm binds and regulates these genes. Y-axis limits are set from -5 to 5 for occupancy comparison across the tracks. The coordinates indicated at the top are in kilobases.

Fig. S4: Temperature shift protocols

(A-C) Show the temperature shift (TS) protocols used in different experiments. Blue lines indicate when the flies were grown at 18°C. Red lines indicate the time for

which the flies were grown at 29°C. Black line indicate the developmental timeline for at 25°C. The black downward facing arrow indicates the time of dissection of the larvae. The L3 stage has been divided into three 16 hr intervals to define the early, mid, and late L3 stage.

Fig. S5: Double knockdown of *Su(H)* and *brm* reduces Cut levels in A8-A10 NBs

(A-D) Show levels of Cut (10.16±3.99, 106 NBs, *n*=7 VNCs *N* = 3) (A), in control A8-A10 NBs blocked for apoptosis by expression of p35. The Cut expression is significantly reduced in A8-A10 NBs upon the knockdown of Su(H) (*Su(H)-RNAi;* 5.17±2.39, 91 NBs, *n*=8 VNCs *N* = 3) (B) and double knockdown for Su(H) and Brm (*Su(H)-RNAi* and *brm-RNAi*; 3.39±1.08, 107 NBs, *n* = 8 VNCs, *N* = 3) (D), but not in case of Brm knockdown alone (*brm-RNAi*; 9.74±3.51, 101 NBs, *n* = 15 VNCs, *N* = 3) (C), in the late L3 stage. (E) Graph comparing the levels of Cut in control, single knockdown for *Brm* and Su(H)*;* and double knockdown for the two together. Yellow arrowheads indicate the ectopic NBs. Scale bars are 10 µm. Graph shows mean±SD. Significance is from a two-tailed Students' unpaired *t-test*.

Materials and Methods

Fly stocks:

Following lines were used: *Canton-S* (BDSC 64349), *brm-RNAi* (BDSC 31712, VDRC 37720, VDRC 37721), *Delta*-RNAi (BDSC 36784), *Notch*-RNAi (BDSC 28981), *Su(H)*-RNAi (BDSC 28900, VDRC 103597), *nej-RNAi* (BDSC 27724, BDSC 37489), *UAS-HA-hSMARCA2* (BDSC 84943), $N^{[55e11]}$ (BDSC 28813), brm^{d00415} (BDSC 19144), $brm^{[I21]}$ (BDSC 4108), brm^{2} (BDSC 3619), brm^{K804R} (Well Genetics for this study). *UAS-HA-brm* (this study), *UAS-HA-brm*-K804R (this study), *UAS-p35* (DGRC 108019), *UAS-dcr2; inscGAL4 UASmCD8-GFP and UAS-dcr2; inscGAL4 UASmCD8-GFP; tub-GAL80^{ts} (*J. A. Knoblich), *worniu-GAL4* (C. Doe), *UAS-LT3-Dam, UAS-LT3-Dam-Brm* (A. Brand [44]), *E(spl)mγ-GFP* (S. Bray [42]), *F3B3-LacZ* [20], *Δ717* [22].

CRISPR-mediated mutagenesis for *brm*^{K804R} allele was performed by WellGenetics Inc. using modified methods of Kondo and Ueda [49]. In brief, gRNA sequence AAGGTAGGTTACCAGCGAAA[TGG] were cloned into U6 promoter plasmid(s). Cassette PBacDsRed, which contains 3xP3-DsRed flanked by PiggyBac terminal repeats, and two homology arms with point mutation were cloned into pUC57-Kan as donor template for repair. *brm*-targeting gRNAs and hs-Cas9 were supplied in DNA plasmids, together with donor plasmid for microinjection into embryos of control strain *w*$^{[1118]}$. F1 flies carrying selection marker of 3xP3-DsRed were further validated by genomic PCR and sequencing. CRISPR generates a break in *brm* and is replaced by cassette PBacDsRed with the point mutation in the upstream homolog arm. Thereafter, the PBacDsRed is excised out, leaving behind the point mutation at the endogenous locus. Point mutation was further confirmed by isolating genomic DNA from a single fly and performing Sanger sequencing.

Fly husbandry:

All the fly stocks and crosses were maintained at 25°C. Egg collection were done in 6 hours' window and the larvae were reared at 25°C (for mutants) or 29°C (for RNAi knockdown/overexpression/rescue experiments) until dissection. Details of the genotypes analysed in each figure are given in the supplementary data.

RNA interference experiments:

Virgin females of *UAS-dcr2; inscGAL4-UASmCD8-GFP* were crossed to the flies of the following genotypes and progeny of the required genotypes were separated and dissected: *Canton-S, UAS-brm-RNAi, UAS-HA-brm-K804R, UAS-Su(H)-RNAi, UAS-Notch-RNAi, UAS-mam-RNAi, UAS-Dl-RNAi, UAS-Nej-RNAi, UAS-HA-brm, UAS-Moira-RNAi, UAS-Snr1-RNAi, UAS-Bap111-RNAi, UAS-Bap55-RNAi, UAS-Osa-RNAi, UAS-SayP-RNAi, UAS-mam-RNAi, UAS-Polybromo-RNAi, UAS-Bap170-RNAi*.

Six-hour egg collections were done, and the embryos were reared at 25°C for 24 hours before shifting to 29°C till late L3 stage dissection, when the larvae were sexed, separated, and subsequently dissected. The effect of these knockdowns on *F3B3-lacZ* was checked in A8-A10 NBs and was quantified and compared to lacZ levels in A8-A10 NBs that have been blocked for apoptosis by expression of p35 (which served as a control). For *UAS-p35* control experiments, virgin females of *UAS-dcr2; inscGAL4 UASmCD8-GFP; tub-GAL80*^{ts} were crossed to the *UAS-p35* flies, and larvae were reared at 18°C for 48-54 hours and then shifted to 29°C until dissection at the LL3 stage. The schematic of the temperature-shift (TS) protocol for these experiments is summarised in Fig. S4C.

Immunostaining staining image acquisition:

Larvae of Late L3 stage of desirable sex were dissected and fixed in 4% paraformaldehyde in 1X PBS and 0.1% TritonX-100 for 30 minutes at room temperature. The following primary antibodies were used: rabbit anti-*Dpn*, 1:2000; rat anti-*Dpn*, 1:1000; rabbit anti-*Grh*, 1:2000, mouse Abd-B (1:500, 1A2E9, DSHB), mouse anti-*NICD* (1:50, C17.9C6, DHSB), mouse anti-*Dl* (1:10, C594.9B, DHSB), mouse anti-*Ct* (1:500, 2B10, DHSB), chicken anti-GFP (1:2000, ab13970, Abcam),

chicken anti-β-gal (1:2000, ab9361, Abcam), chicken anti-HA (1:500, ab9111, Abcam), mouse anti-*mam* (1:1000 PMID: 8725234), rat anti-*nej* (1:1000 PMID: 19075001), mouse anti-*Su(H)* (1:500, SC-398453, Santa-Cruz), Rabbit anti-*H3K27ac* (1:1000, ab4729, Abcam). Secondary antibodies conjugated to Alexa fluorophores from Molecular Probes were used: AlexaFluor-405 (1:250); AlexaFluor-488 (1:500); AlexaFluor-555 (1:1000); and AlexaFluor-647 (1:250). The samples were mounted in 70% glycerol and images were acquired with Zeiss LSM 700 and LSM 900 confocal microscopes and processed using ImageJ and Adobe Illustrator CS3. Scale bars are shown in figure legends. Microsoft Excel and GraphPad Prism was used for all the data analysis (unpaired student t-test was done to check significance of the data). At least three technical replicates were done for all the experiments. A minimum of seven VNCs were analyzed across these replicates, and a representative confocal image is shown for each experiment.

RNA isolation, reverse transcription and qRT-PCR:

RNA extraction was done using 50-60 L3 larval brains of suitable genotype. TRIzol (Thermo Fisher #15596018) was used, followed by chloroform extraction and isopropanol precipitation. Thereafter RNA was resuspended in RNase free water. For reverse transcription, RNA was treated with DNase (Invitrogen TURBO DNA-free kit AM1907) and then converted to cDNA using Takara cDNA synthesis kit (PrimeScript cDNA Synthesis Kit #6110A). cDNA was diluted five-fold before using for qRT-PCR. cDNA was then subjected to qRT-PCR using Takara SYBR Green (TB Green Premix Ex Taq, ROX Plus #RR42LR) in Himedia LA1074-1NO Insta Q96 - 6.0. Transcript levels were quantified using $2^{-\Delta\Delta Ct}$ method [50], and transcript levels were normalized using GAPDH. Primer sequences are provided in the supplementary data.

Dam-ID and qRT-PCR:

We used NB-specific *inscGAL4* to drive the expression of very low levels of Dam-Brm fusion protein and Dam protein alone. The Brm binding in the genome was assayed by methylation of nearby GATC sequences and normalised over baseline GATC methylation carried out by Dam alone, using RT-PCR.

To check *Brm* binding on 1kb apoptotic enhancer, *UAS-LT3-Dam* and *UAS-LT3-DamBrm* flies [44] were crossed to *UAS-dcr2; inscGAL4 UASmCD8-GFP; tub-GAL80^{ts}* virgin female flies. Six hour egg collection was done in 25°C embryos were shifted and reared at 18°C until mL2 stage and then shifted to 29°C (TS as shown in the Fig. S4B). 50-60 brains with VNC from mL3 stage were dissected and collected in 1X PBS and stored in -80°C until used. The tissues were processed as per the published Targeted DamID protocol [51], where genomic DNA was extracted from control and test tissues, digested with Dpn I, followed by adapter ligation and Dpn II digest, thereafter PCR amplification and sonication was done. Subsequently, adaptors were removed, and the sonicated genomic samples were subjected to qRT-PCR. The samples were diluted five-fold before qRT-PCR. Fold enrichment in case of Dam-Brm on *F3B3* was compared to Dam-only using formula $2^{Ct\ (Dam\text{-}only)\ -\ Ct\ (Dam\text{-}Brm)}$. Sequence of the *F3B3* specific primers used are given in the supplementary data.

***In vitro* GST-pulldown:**

The following proteins were used for *in vitro* pulldown: GST-Su(H), 6X His-Brm F1 (1-311aa), His-Brm F2 (304-747aa) and His-Brm F3 (748-1638aa). Bacterial cultures expressing full length GST-tagged *Su(H)* and GST-only were induced for 4 hours with 0.5 mM IPTG at 18°C and different fragments of His-tagged Brm proteins were induced for 4 hours with 0.25mM IPTG at 37°C. After sonication, lysates were treated with Micrococcal Nuclease (MN) at 37°C for half an hour. GST-Su(H) and GST-only were incubated with GST beads for 2 h at 4°C. Overnight IP was set with bead-bound GST-Su(H) and GST-only and His-tagged Brm F1, F2 and F3 lysates. Bead-bound proteins were separated by denaturing SDS-PAGE and then transferred onto PVDF membranes. The membrane was blocked in 5% milk in Tris-buffered saline with 0.1% Tween 20 (TBST). Primary antibody-mouse anti-His (H1029; Sigma-Aldrich) was diluted 1 in 5000 in 5% milk in TBST, and the blot was incubated overnight at 4°C. HRP conjugated secondary antibody (Peroxidase-AffiniPure Rabbit Anti-Mouse IgG + IgM(H + L) (1/10,000, 315-035-048; Jackson Immunological Research Laboratory, USA) was used. Visualization was carried out by Enhanced Chemiluminescent femtoLUCENT PLUS HRP chemiluminescent detection (G Biosciences #786003) in Intelligent ImageQuant LAS 500. Representative blots from at least 3 repetitions of the experiments are shown in the figures.

In vivo pulldown assays with whole larvae:

50 larvae were homgenized and lysed in RIPA buffer (150mM NaCl, 10mM Tris-HCl pH 7.5, 1mM EDTA, 0.1% Triton X-100, 0.1% SDS, 0.1% Sodium deoxycholate, 1mM PMSF and Protease Inhibitor). Protein A beads were incubated with Rabbit Anti-IgG (Merck 12-370, Lot #2378704) and Rabbit Anti-Brm [40] for 5 hours at 4°C. Pre-cleaned lysates were then set for overnight IP with protein A beads bound to Rabbit Anti-IgG and Rabbit Anti-Brm. Next day beads were washed and a denaturing SDS-PAGE was run. Proteins were then transferred to PVDF membrane and membrane was blocked in 5% milk in Tris-buffered saline with 0.1% Tween 20 (TBST). Primary antibody, mouse anti-mam (1:1000;[52]), rat anti-*nej* (1:1000; [53]), and rat anti-Su(H) (1:2000, MABE982, Merck) were diluted in 5% milk in TBST and incubated overnight at 4°C. HRP conjugated secondary antibody Peroxidase-AffiniPure Rabbit Anti-Mouse IgG + IgM(H + L) (1:10,000, 315-035-048; Jackson Immunological Research Laboratory, USA), Peroxidase AffiniPure Goat Anti-Rat IgG (H+L) (1:10,000, 112-035-003; Jackson Immunological Research Laboratory, USA) were used. Visualization was carried out by Enhanced Chemiluminescent femtoLUCENT PLUS HRP chemiluminescent detection (G Biosciences #786003) in Intelligent ImageQuant LAS 500. Representative blots from at least three repetitions of the experiments are shown in the figures.

Acknowledgements

We thank C. Doe, J. Knoblich, A. Brand for reagents; BDSC, VDRC, NIG-Fly, and DGRC -Japan stock centres for fly lines; CDFD animal facility, Bioklone Biotech Pvt. Ltd., Chennai and the Developmental Studies Hybridoma Bank at The University of Iowa for antibodies and TFF at NCBS-CCAMP, Bangalore for transgenic flies. We thank Raviranjan Kumar for making initial observations with Brahma knockdown lines, Prakeerthi Abburi for help with generation of Pygenome tracks for Targeted DamID data (published by Marshall and Brand, 2017) showing Brm binding on different genes for Figure S6 showing and C. S. Singh for his assistance in various

phases of the project. This study was funded by; Department of Science and Technology, India (CRG/2021/003275); Department of Biotechnology, India (BT/PR27455/BRB/10/1647/2018, BT/PR41306/MED/122/ 259/2020 and BT/PR45460/MED/12/952/2022); CDFD core funds; and DST Inspire, India (award to PB) [Reference No IF170651].

Author contribution

RJ conceptualised the study; PB and VP did the experiments; RJ and PB analysed the data; RJ and PB wrote the manuscript.

During the preparation of this work, the author(s) used Grammarly software to check for spelling, grammar, punctuation, clarity, engagement, and delivery mistakes in English text. After using this tool/service, the corresponding author reviewed and edited the content as needed and takes full responsibility for the content of the publication.

References

1. Homem, C.C. and J.A. Knoblich, *Drosophila neuroblasts: a model for stem cell biology.* Development, 2012. **139**(23): p. 4297-310.
2. Doe, C.Q., *Temporal Patterning in the Drosophila CNS.* Annu Rev Cell Dev Biol, 2017. **33**: p. 219-240.
3. Kohwi, M. and C.Q. Doe, *Temporal fate specification and neural progenitor competence during development.* Nat Rev Neurosci, 2013. **14**(12): p. 823-38.
4. Prokop, A., et al., *Homeotic regulation of segment-specific differences in neuroblast numbers and proliferation in the Drosophila central nervous system.* Mech Dev, 1998. **74**(1-2): p. 99-110.
5. Economides, K.D., L. Zeltser, and M.R. Capecchi, *Hoxb13 mutations cause overgrowth of caudal spinal cord and tail vertebrae.* Dev Biol, 2003. **256**(2): p. 317-30.
6. Bello, B.C., F. Hirth, and A.P. Gould, *A pulse of the Drosophila Hox protein Abdominal-A schedules the end of neural proliferation via neuroblast apoptosis.* Neuron, 2003. **37**(2): p. 209-19.
7. Dasen, J.S., J.P. Liu, and T.M. Jessell, *Motor neuron columnar fate imposed by sequential phases of Hox-c activity.* Nature, 2003. **425**(6961): p. 926-33.
8. Miguel-Aliaga, I. and S. Thor, *Segment-specific prevention of pioneer neuron apoptosis by cell-autonomous, postmitotic Hox gene activity.* Development, 2004. **131**(24): p. 6093-105.
9. Dasen, J.S., et al., *A Hox regulatory network establishes motor neuron pool identity and target-muscle connectivity.* Cell, 2005. **123**(3): p. 477-91.
10. Rogulja-Ortmann, A., S. Renner, and G.M. Technau, *Antagonistic roles for Ultrabithorax and Antennapedia in regulating segment-specific apoptosis of differentiated motoneurons in the Drosophila embryonic central nervous system.* Development, 2008. **135**(20): p. 3435-45.
11. Tabuse, M., et al., *Functional analysis of HOXD9 in human gliomas and glioma cancer stem cells.* Mol Cancer, 2011. **10**: p. 60.
12. Suska, A., I. Miguel-Aliaga, and S. Thor, *Segment-specific generation of Drosophila Capability neuropeptide neurons by multi-faceted Hox cues.* Dev Biol, 2011. **353**(1): p. 72-80.

13. Kuert, P.A., B.C. Bello, and H. Reichert, *The labial gene is required to terminate proliferation of identified neuroblasts in postembryonic development of the Drosophila brain.* Biol Open, 2012. **1**(10): p. 1006-15.
14. Birkholz, O., et al., *Neuroblast pattern and identity in the Drosophila tail region and role of doublesex in the survival of sex-specific precursors.* Development, 2013. **140**(8): p. 1830-42.
15. Baek, M., J. Enriquez, and R.S. Mann, *Dual role for Hox genes and Hox co-factors in conferring leg motoneuron survival and identity in Drosophila.* Development, 2013. **140**(9): p. 2027-38.
16. Kocak, H., et al., *Hox-C9 activates the intrinsic pathway of apoptosis and is associated with spontaneous regression in neuroblastoma.* Cell Death Dis, 2013. **4**: p. e586.
17. Kuert, P.A., et al., *Neuroblast lineage identification and lineage-specific Hox gene action during postembryonic development of the subesophageal ganglion in the Drosophila central brain.* Dev Biol, 2014. **390**(2): p. 102-15.
18. Moris-Sanz, M., et al., *The study of the Bithorax-complex genes in patterning CCAP neurons reveals a temporal control of neuronal differentiation by Abd-B.* Biol Open, 2015. **4**(9): p. 1132-42.
19. Arya, R., et al., *Neural stem cell progeny regulate stem cell death in a Notch and Hox dependent manner.* Cell Death Differ, 2015. **22**(8): p. 1378-87.
20. Khandelwal, R., et al., *Combinatorial action of Grainyhead, Extradenticle and Notch in regulating Hox mediated apoptosis in Drosophila larval CNS.* PLoS Genet, 2017. **13**(10): p. e1007043.
21. Ghosh, N., et al., *The Hox gene Abdominal-B uses Doublesex(F) as a cofactor to promote neuroblast apoptosis in the Drosophila central nervous system.* Development, 2019. **146**(16).
22. Bakshi, A., et al., *Sequential activation of Notch and Grainyhead gives apoptotic competence to Abdominal-B expressing larval neuroblasts in Drosophila Central nervous system.* PLoS Genet, 2020. **16**(8): p. e1008976.
23. Sipani, R. and R. Joshi, *Hox genes collaborate with helix-loop-helix factor Grainyhead to promote neuroblast apoptosis along the anterior-posterior axis of the Drosophila larval central nervous system.* Genetics, 2022. **222**(1).
24. Yamaguchi, Y. and M. Miura, *Programmed Cell Death and Caspase Functions During Neural Development.* Curr Top Dev Biol, 2015. **114**: p. 159-84.
25. Yamaguchi, Y. and M. Miura, *Programmed cell death in neurodevelopment.* Dev Cell, 2015. **32**(4): p. 478-90.
26. Pinto-Teixeira, F., N. Konstantinides, and C. Desplan, *Programmed cell death acts at different stages of Drosophila neurodevelopment to shape the central nervous system.* FEBS Lett, 2016. **590**(15): p. 2435-2453.
27. Truman, J.W. and M. Bate, *Spatial and temporal patterns of neurogenesis in the central nervous system of Drosophila melanogaster.* Dev Biol, 1988. **125**(1): p. 145-57.
28. Yeo, W. and J. Gautier, *Early neural cell death: dying to become neurons.* Dev Biol, 2004. **274**(2): p. 233-44.
29. Cenci, C. and A.P. Gould, *Drosophila Grainyhead specifies late programmes of neural proliferation by regulating the mitotic activity and Hox-dependent apoptosis of neuroblasts.* Development, 2005. **132**(17): p. 3835-45.
30. Quaggin, S.E., H. Yeger, and P. Igarashi, *Antisense oligonucleotides to Cux-1, a Cut-related homeobox gene, cause increased apoptosis in mouse embryonic kidney cultures.* J Clin Invest, 1997. **99**(4): p. 718-24.
31. Barkett, M. and T.D. Gilmore, *Control of apoptosis by Rel/NF-kappaB transcription factors.* Oncogene, 1999. **18**(49): p. 6910-24.
32. Grether, M.E., et al., *The head involution defective gene of Drosophila melanogaster functions in programmed cell death.* Genes Dev, 1995. **9**(14): p. 1694-708.

33. White, K., et al., *Genetic control of programmed cell death in Drosophila.* Science, 1994. **264**(5159): p. 677-83.
34. Bray, S.J., *Notch signalling in context.* Nat Rev Mol Cell Biol, 2016. **17**(11): p. 722-735.
35. Skalska, L., et al., *Chromatin signatures at Notch-regulated enhancers reveal large-scale changes in H3K56ac upon activation.* EMBO J, 2015. **34**(14): p. 1889-904.
36. Pillidge, Z. and S.J. Bray, *SWI/SNF chromatin remodeling controls Notch-responsive enhancer accessibility.* EMBO Rep, 2019. **20**(5).
37. Niederhuber, M.J., M. Leatham-Jensen, and D.J. McKay, *The SWI/SNF nucleosome remodeler constrains enhancer activity during Drosophila wing development.* Genetics, 2024. **226**(2).
38. Armstrong, J.A., et al., *Genetic screens for enhancers of brahma reveal functional interactions between the BRM chromatin-remodeling complex and the delta-notch signal transduction pathway in Drosophila.* Genetics, 2005. **170**(4): p. 1761-74.
39. Armstrong, J.A., et al., *The Drosophila BRM complex facilitates global transcription by RNA polymerase II.* EMBO J, 2002. **21**(19): p. 5245-54.
40. Elfring, L.K., et al., *Genetic analysis of brahma: the Drosophila homolog of the yeast chromatin remodeling factor SWI2/SNF2.* Genetics, 1998. **148**(1): p. 251-65.
41. Tamkun, J.W., et al., *brahma: a regulator of Drosophila homeotic genes structurally related to the yeast transcriptional activator SNF2/SWI2.* Cell, 1992. **68**(3): p. 561-72.
42. Almeida, M.S. and S.J. Bray, *Regulation of post-embryonic neuroblasts by Drosophila Grainyhead.* Mech Dev, 2005. **122**(12): p. 1282-93.
43. Southall, T.D., et al., *Regulation of self-renewal and differentiation in the Drosophila nervous system.* Cold Spring Harb Symp Quant Biol, 2008. **73**: p. 523-8.
44. Marshall, O.J. and A.H. Brand, *Chromatin state changes during neural development revealed by in vivo cell-type specific profiling.* Nat Commun, 2017. **8**(1): p. 2271.
45. Hong, S.T. and K.W. Choi, *Antagonistic roles of Drosophila Tctp and Brahma in chromatin remodelling and stabilizing repeated sequences.* Nat Commun, 2016. **7**: p. 12988.
46. Allen, M.D., M. Bycroft, and G. Zinzalla, *Structure of the BRK domain of the SWI/SNF chromatin remodeling complex subunit BRG1 reveals a potential role in protein-protein interactions.* Protein Sci, 2020. **29**(4): p. 1047-1053.
47. Trotter, K.W., et al., *The HSA domain of BRG1 mediates critical interactions required for glucocorticoid receptor-dependent transcriptional activation in vivo.* Mol Cell Biol, 2008. **28**(4): p. 1413-26.
48. Tie, F., et al., *Histone demethylase UTX and chromatin remodeler BRM bind directly to CBP and modulate acetylation of histone H3 lysine 27.* Mol Cell Biol, 2012. **32**(12): p. 2323-34.
49. Kondo, S. and R. Ueda, *Highly improved gene targeting by germline-specific Cas9 expression in Drosophila.* Genetics, 2013. **195**(3): p. 715-21.
50. Livak, K.J. and T.D. Schmittgen, *Analysis of relative gene expression data using real-time quantitative PCR and the 2(-Delta Delta C(T)) Method.* Methods, 2001. **25**(4): p. 402-8.
51. Marshall, O.J., et al., *Cell-type-specific profiling of protein-DNA interactions without cell isolation using targeted DamID with next-generation sequencing.* Nat Protoc, 2016. **11**(9): p. 1586-98.
52. Bettler, D., S. Pearson, and B. Yedvobnick, *The nuclear protein encoded by the Drosophila neurogenic gene mastermind is widely expressed and associates with specific chromosomal regions.* Genetics, 1996. **143**(2): p. 859-75.
53. Zhao, Y., et al., *Corepressive action of CBP on androgen receptor transactivation in pericentric heterochromatin in a Drosophila experimental model system.* Mol Cell Biol, 2009. **29**(4): p. 1017-34.

Figure 1

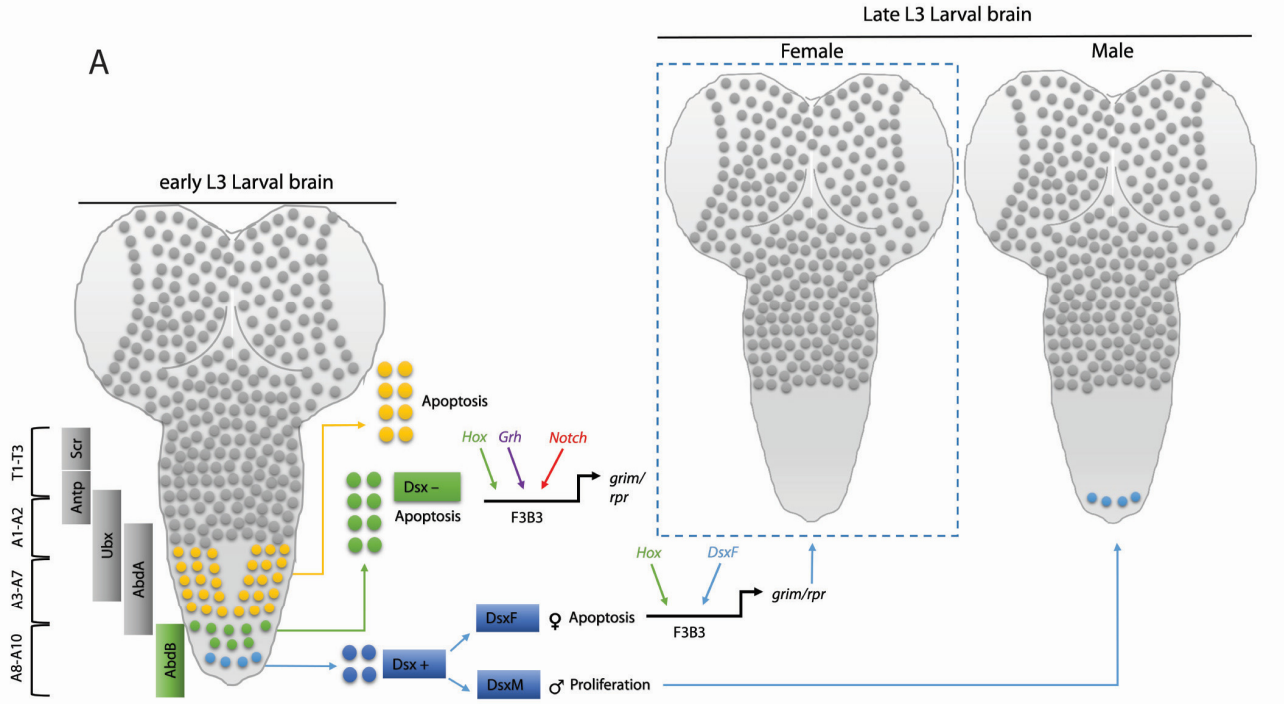
A
early L3 Late L3 Larval brain
Female
Male
Apoptosis
Hox Grh Notch
Dsx –
Apoptosis
grim/ rpr
F3B3
Hox DsxF
grim/rpr
F3B3
DsxF ♀ Apoptosis
Dsx +
DsxM ♂ Proliferation
Scr
Antp
Ubx
AbdA
AbdB
T1-T3
A1-A2
A3-A7
A8-A10

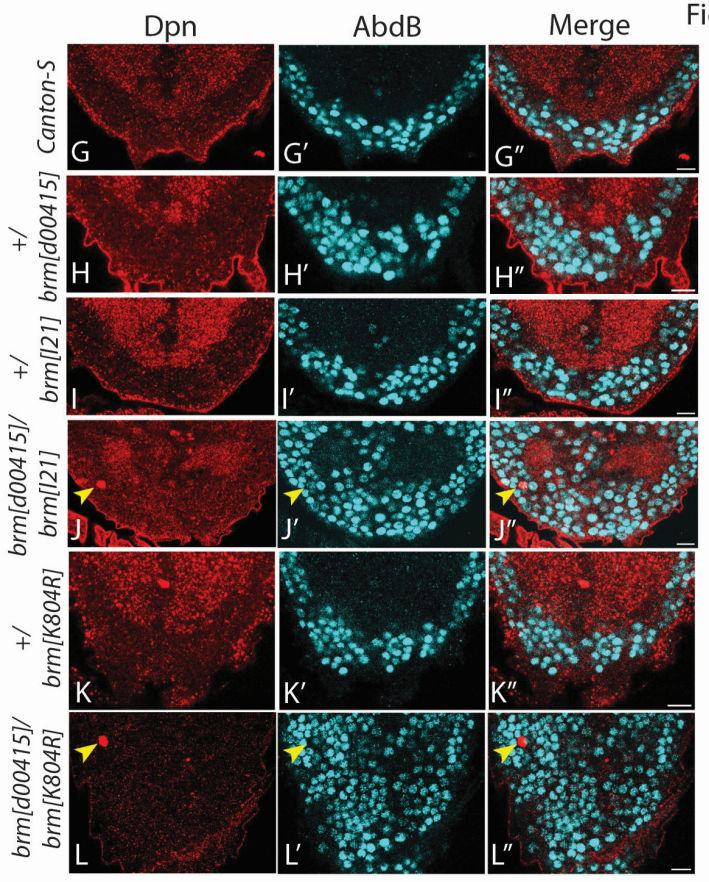
Dpn
AbdB
Merge
Canton-S
+/ brm[d00415]
+/ brm[I21]
brm[d00415]/ brm[I21]
+/ brm[K804R]
brm[d00415]/ brm[K804R]
G G′ G″
H H′ H″
I I′ I″
J J′ J″
K K′ K″
L L′ L″
Single z-slice, 114-120 hrs AEL, A8-A10 segment of female CNS larvae

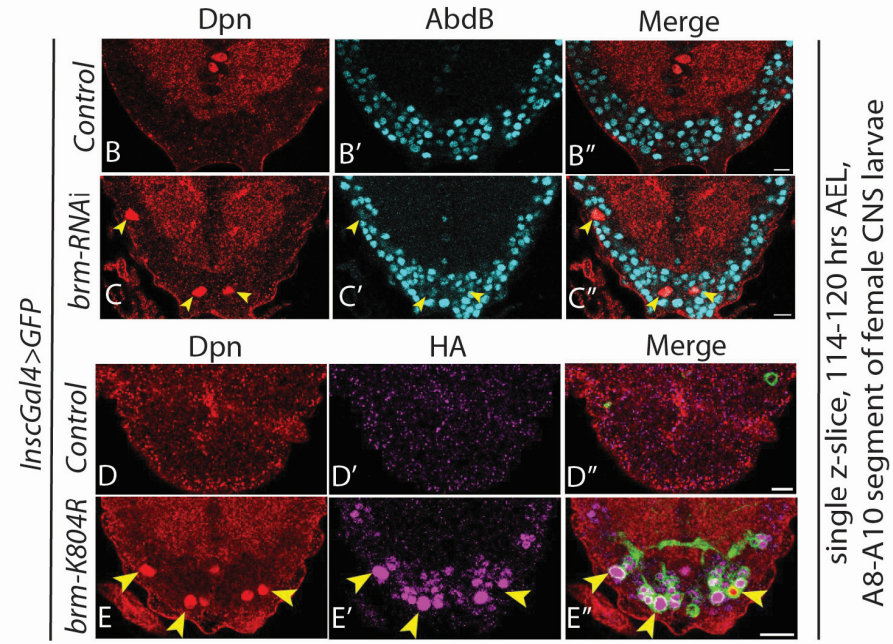
Dpn
AbdB
Merge
Control
brm-RNAi
B B′ B″
C C′ C″
Dpn
HA
Merge
Control
brm-K804R
D D′ D″
E E′ E″
InscGal4>GFP
single z-slice, 114-120 hrs AEL, A8-A10 segment of female CNS larvae

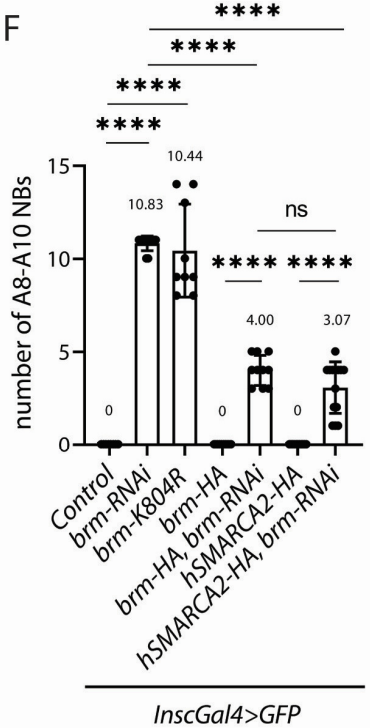
F
number of A8-A10 NBs
0
5
10
15
0
10.83
10.44
0
4.00
0
3.07
****
****
****
****
****
****
ns
Control
brm-RNAi
brm-K804R
brm-HA
brm-HA, brm-RNAi
hSMARCA2-HA
hSMARCA2-HA, brm-RNAi
InscGal4>GFP

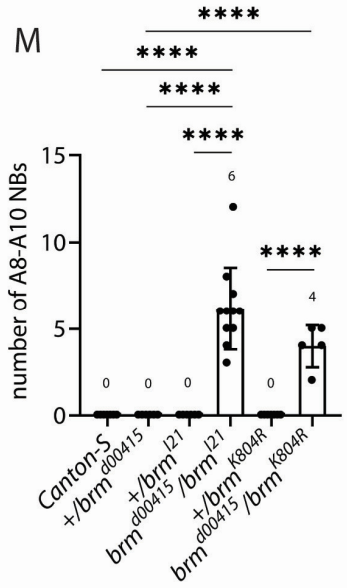
M
number of A8-A10 NBs
0
5
10
15
0
0
0
6
0
4
****
****
****
****
****
Canton-S
+/brm d00415
+/brm d00415 /brm I21
+/brm I21
+/brm d00415 /brm K804R
+/brm K804R

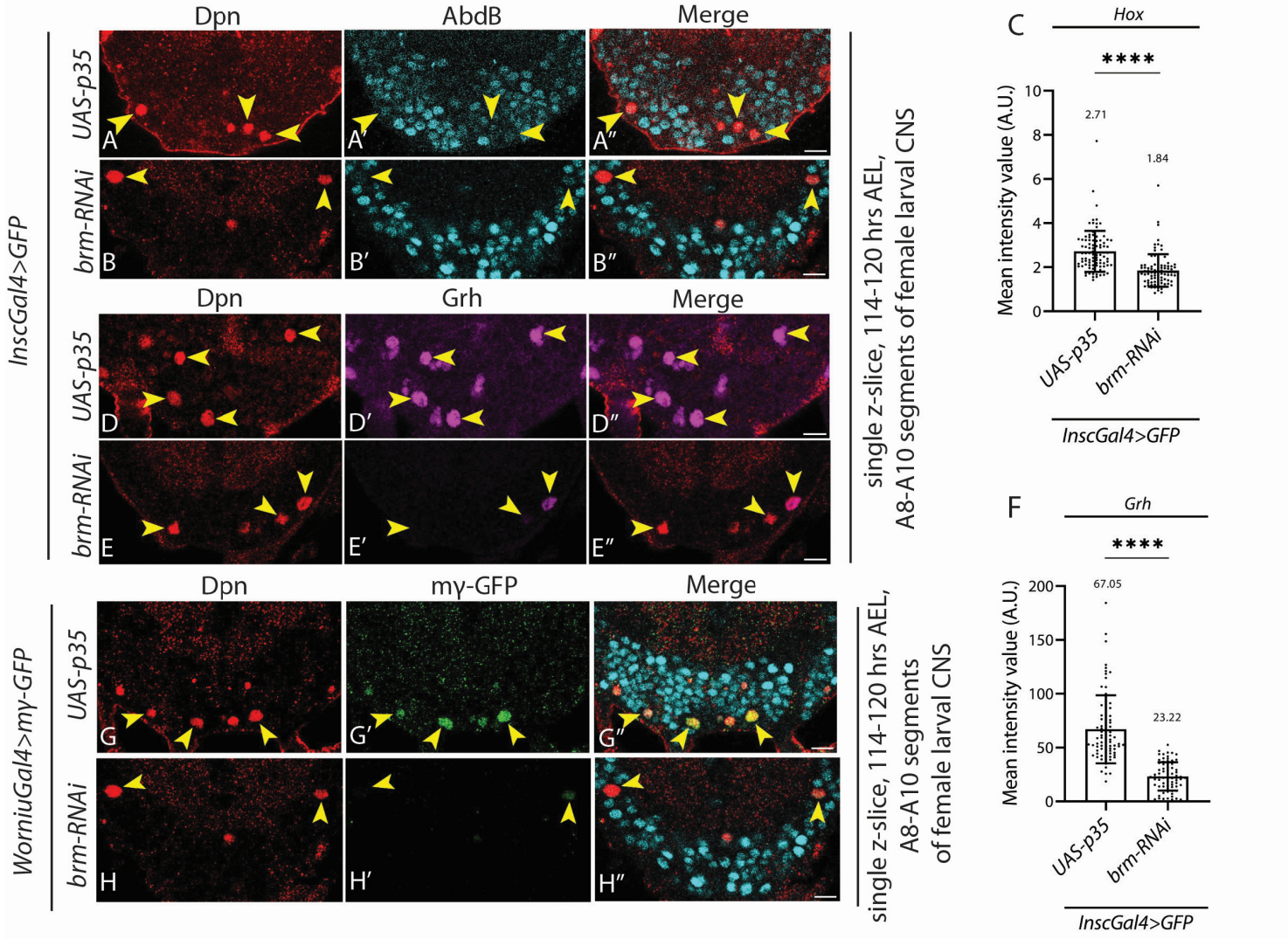
Dpn
AbdB
Merge
InscGal4>GFP
UAS-p35
brm-RNAi
A
A′
A″
B
B′
B″
Dpn
Grh
Merge
D
D′
D″
E
E′
E″
single z-slice, 114-120 hrs AEL, A8-A10 segments of female larval CNS
C
Hox
****
Mean intensity value (A.U.)
2.71
1.84
UAS-p35
brm-RNAi
InscGal4>GFP
F
Grh
****
67.05
23.22
WorniuGal4>mγ-GFP
Dpn
mγ-GFP
Merge
G
G′
G″
H
H′
H″
single z-slice, 114-120 hrs AEL, A8-A10 segments of female larval CNS

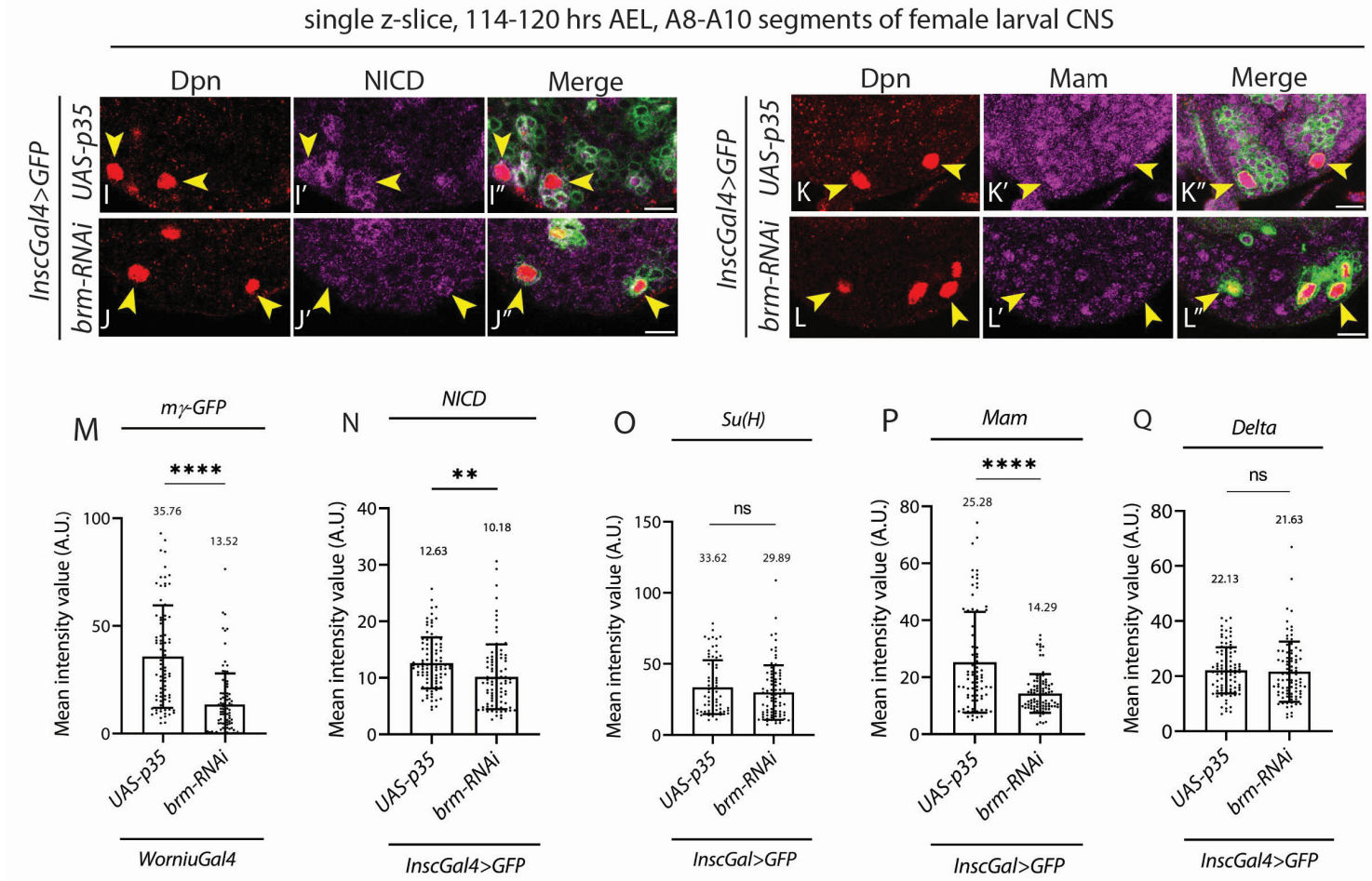
single z-slice, 114-120 hrs AEL, A8-A10 segments of female larval CNS
Dpn
NICD
Merge
Dpn
Mam
Merge
InscGal4>GFP
UAS-p35
brm-RNAi
I
I′
I″
J
J′
J″
K
K′
K″
L
L′
L″
M
mγ-GFP
****
35.76
13.52
N
NICD
**
12.63
10.18
O
Su(H)
ns
33.62
29.89
P
Mam
****
25.28
14.29
Q
Delta
ns
22.13
21.63
Mean intensity value (A.U.)
UAS-p35
brm-RNAi
WorniuGal4
InscGal4>GFP
InscGal>GFP
InscGal>GFP
InscGal4>GFP

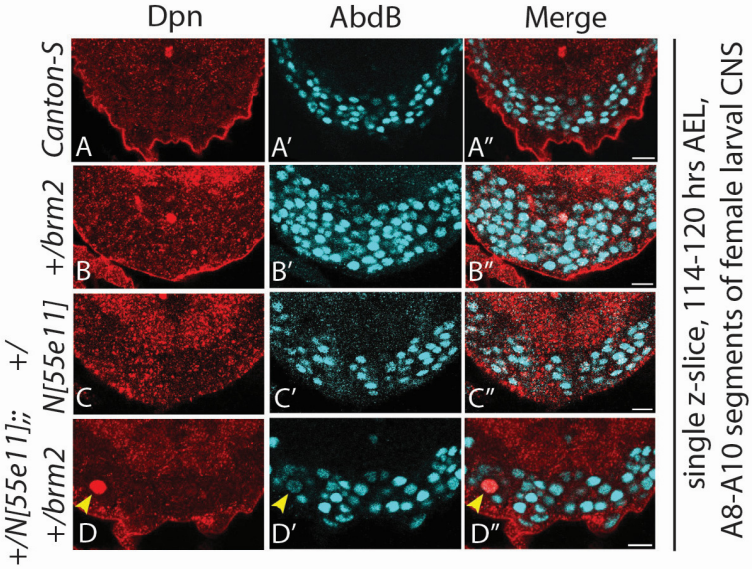
Dpn
AbdB
Merge
Canton-S
+/brm2
+/N[55e11]
+/N[55e11];;+/brm2
A
A′
A″
B
B′
B″
C
C′
C″
D
D′
D″
single z-slice, 114-120 hrs AEL, A8-A10 segments of female larval CNS

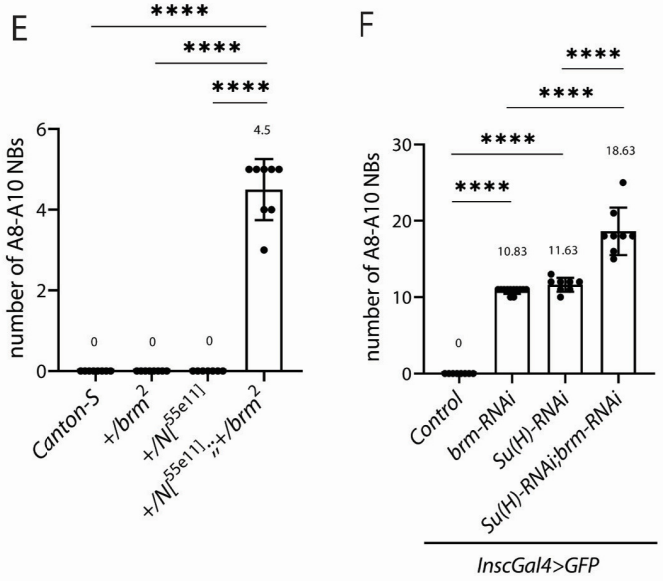
E
number of A8-A10 NBs
0
0
0
4.5
Canton-S
+/brm2
+/N[55e11]
+/N[55e11];;+/brm2
F
number of A8-A10 NBs
0
10.83
11.63
18.63
Control
brm-RNAi
Su(H)-RNAi
Su(H)-RNAi;brm-RNAi
InscGal4>GFP

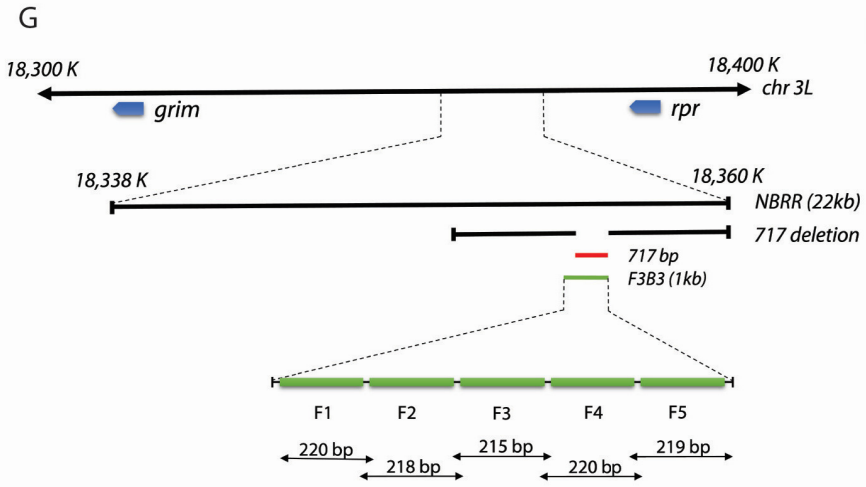
G
18,300 K
18,400 K
chr 3L
grim
rpr
18,338 K
18,360 K
NBRR (22kb)
717 deletion
717 bp
F3B3 (1kb)
F1
F2
F3
F4
F5
220 bp
218 bp
215 bp
220 bp
219 bp

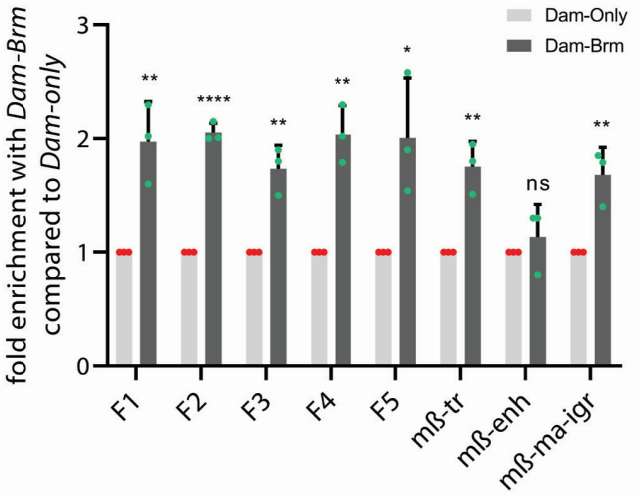
I
Dam-Only
Dam-Brm
fold enrichment with Dam-Brm compared to Dam-only
F1
F2
F3
F4
F5
mß-tr
mß-enh
mß-ma-igr
ns

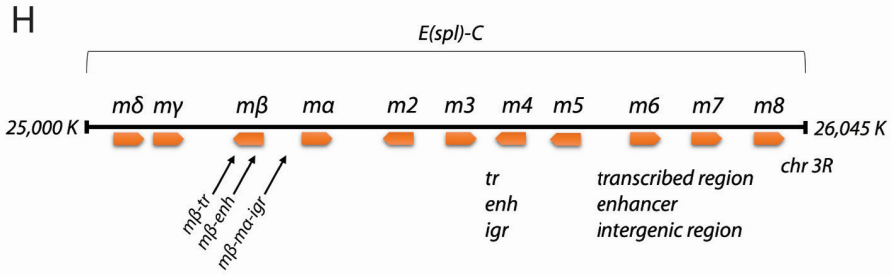
H
E(spl)-C
mδ
mγ
mβ
mα
m2
m3
m4
m5
m6
m7
m8
25,000 K
26,045 K
chr 3R
mß-tr
mß-enh
mß-ma-igr
tr
enh
igr
transcribed region
enhancer
intergenic region

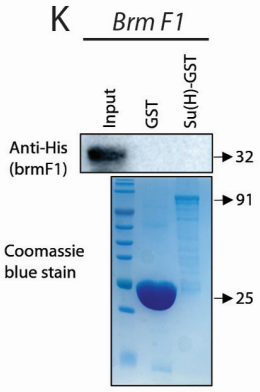
K
Brm F1
Input
GST
Su(H)-GST
Anti-His (brmF1)
32
91
Coomassie blue stain
25

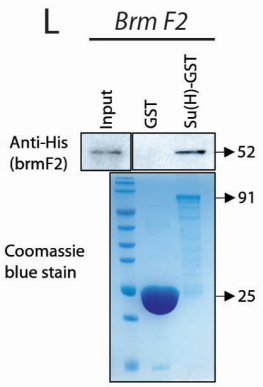
L
Brm F2
Input
GST
Su(H)-GST
Anti-His (brmF2)
52
91
Coomassie blue stain
25

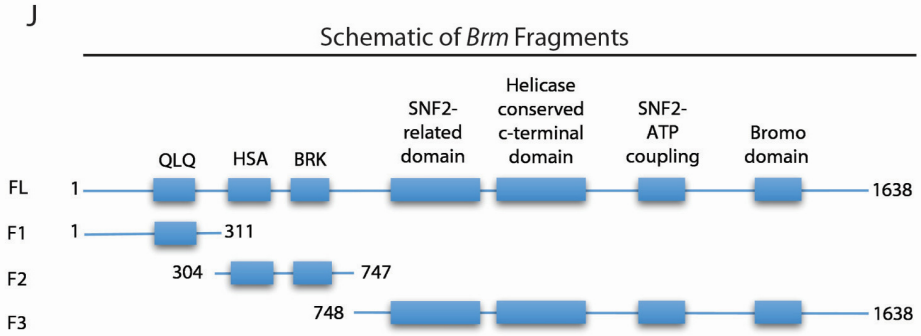
J
Schematic of Brm Fragments
QLQ
HSA
BRK
SNF2-related domain
Helicase conserved c-terminal domain
SNF2-ATP coupling
Bromo domain
FL
1
1638
F1
1
311
F2
304
747
F3
748
1638

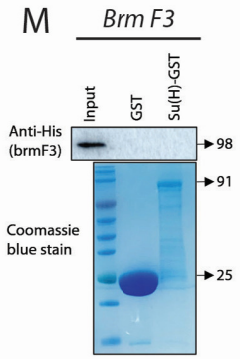
M
Brm F3
Input
GST
Su(H)-GST
Anti-His (brmF3)
98
91
Coomassie blue stain
25

Figure 4

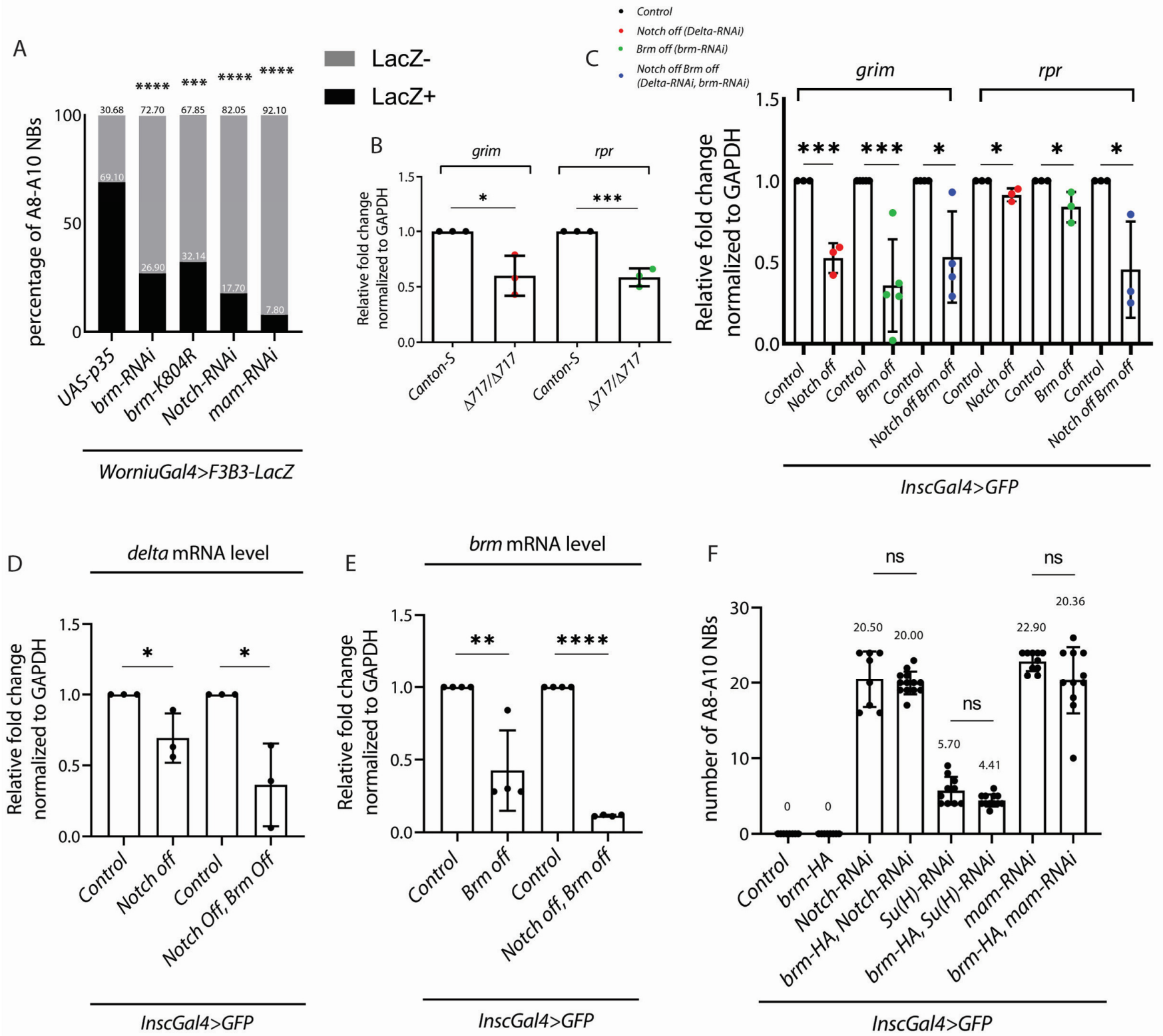
A
LacZ-
LacZ+
percentage of A8-A10 NBs
100
50
0
30.68
72.70
67.85
82.05
92.10
69.10
26.90
32.14
17.70
7.80
****
***
****
****
UAS-p35
brm-RNAi
brm-K804R
Notch-RNAi
mam-RNAi
WorniuGal4>F3B3-LacZ
B
grim
rpr
Relative fold change normalized to GAPDH
1.5
1.0
0.5
0.0
*
***
Canton-S
Δ717/Δ717
Canton-S
Δ717/Δ717
C
Control
Notch off (Delta-RNAi)
Brm off (brm-RNAi)
Notch off Brm off (Delta-RNAi, brm-RNAi)
grim
rpr
Relative fold change normalized to GAPDH
1.5
1.0
0.5
0.0
***
***
*
*
*
*
Control
Notch off
Control
Brm off
Control
Notch off Brm off
Control
Notch off
Control
Brm off
Control
Notch off Brm off
InscGal4>GFP
D
delta mRNA level
Relative fold change normalized to GAPDH
1.5
1.0
0.5
0.0
*
*
Control
Notch off
Control
Notch Off, Brm Off
InscGal4>GFP
E
brm mRNA level
Relative fold change normalized to GAPDH
1.5
1.0
0.5
0.0
**
****
Control
Brm off
Control
Notch off, Brm off
InscGal4>GFP
F
ns
ns
ns
number of A8-A10 NBs
30
20
10
0
0
0
20.50
20.00
5.70
4.41
22.90
20.36
Control
brm-HA
Notch-RNAi
brm-HA, Notch-RNAi
Su(H)-RNAi
brm-HA, Su(H)-RNAi
mam-RNAi
brm-HA, mam-RNAi
InscGal4>GFP

Figure 5

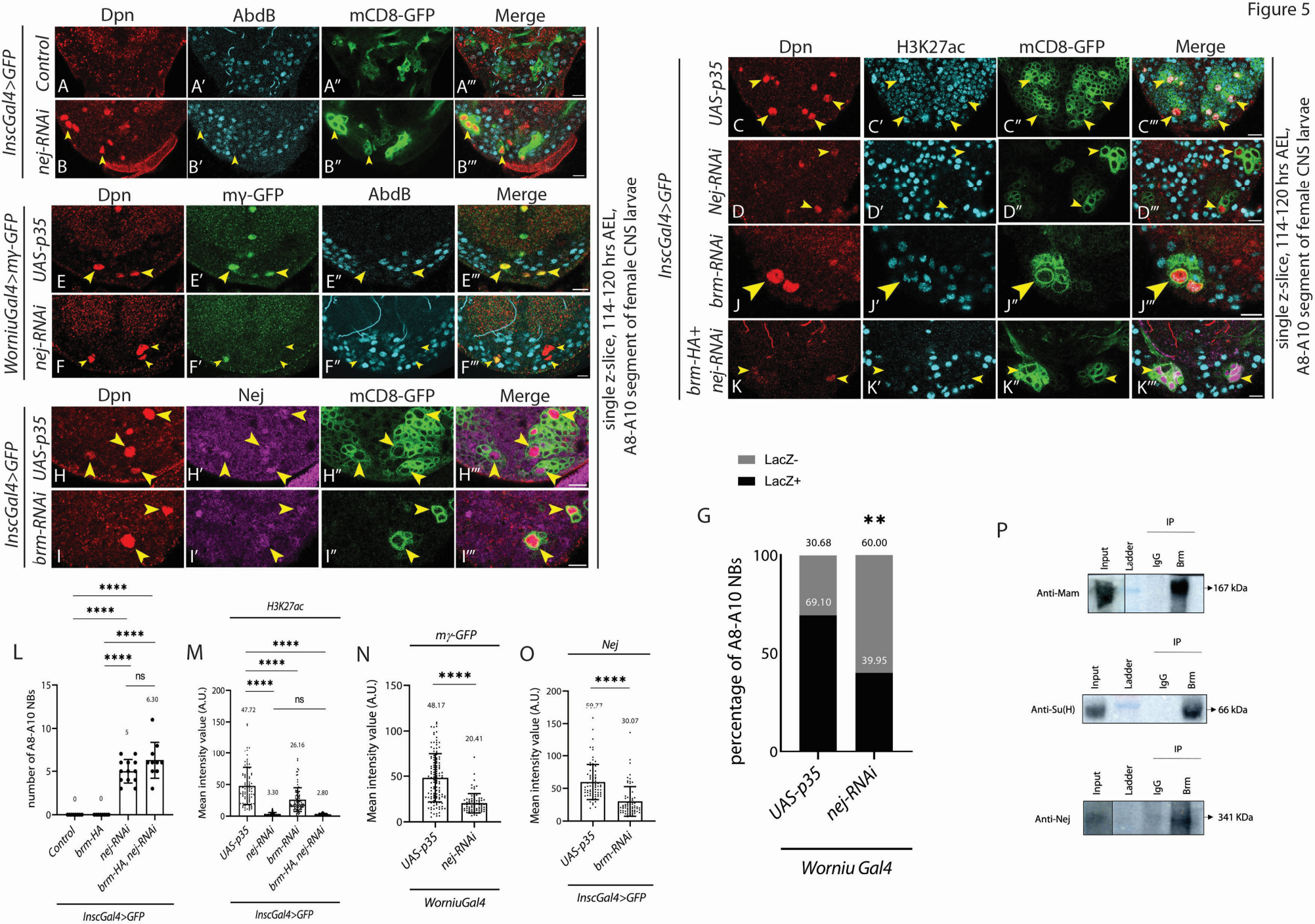
Dpn
AbdB
mCD8-GFP
Merge
InscGal4>GFP
Control
nej-RNAi
A
A′
A″
A‴
B
B′
B″
B‴
Dpn
mγ-GFP
AbdB
Merge
WorniuGal4>mγ-GFP
UAS-p35
nej-RNAi
E
E′
E″
E‴
F
F′
F″
F‴
Dpn
Nej
mCD8-GFP
Merge
InscGal4>GFP
UAS-p35
brm-RNAi
H
H′
H″
H‴
I
I′
I″
I‴
single z-slice, 114-120 hrs AEL,
A8-A10 segment of female CNS larvae
Dpn
H3K27ac
mCD8-GFP
Merge
InscGal4>GFP
UAS-p35
Nej-RNAi
brm-RNAi
brm-HA+
nej-RNAi
C
C′
C″
C‴
D
D′
D″
D‴
J
J′
J″
J‴
K
K′
K″
K‴
single z-slice, 114-120 hrs AEL,
A8-A10 segment of female CNS larvae
LacZ-
LacZ+
G
**
30.68
60.00
69.10
39.95
percentage of A8-A10 NBs
100
50
0
UAS-p35
nej-RNAi
Worniu Gal4
P
IP
Input
Ladder
IgG
Brm
Anti-Mam
167 kDa
Anti-Su(H)
66 kDa
Anti-Nej
341 KDa
L
****
****
****
****
ns
number of A8-A10 NBs
15
10
5
0
0
0
5
6.30
Control
brm-HA
nej-RNAi
brm-HA, nej-RNAi
InscGal4>GFP
M
H3K27ac
****
****
****
ns
Mean intensity value (A.U.)
200
150
100
50
0
47.72
3.30
26.16
2.80
UAS-p35
nej-RNAi
brm-RNAi
brm-HA, nej-RNAi
InscGal4>GFP
N
mγ-GFP
****
Mean intensity value (A.U.)
150
100
50
0
48.17
20.41
UAS-p35
nej-RNAi
WorniuGal4
O
Nej
****
Mean intensity value (A.U.)
200
150
100
50
0
59.77
30.07
UAS-p35
brm-RNAi
InscGal4>GFP

Figure 6

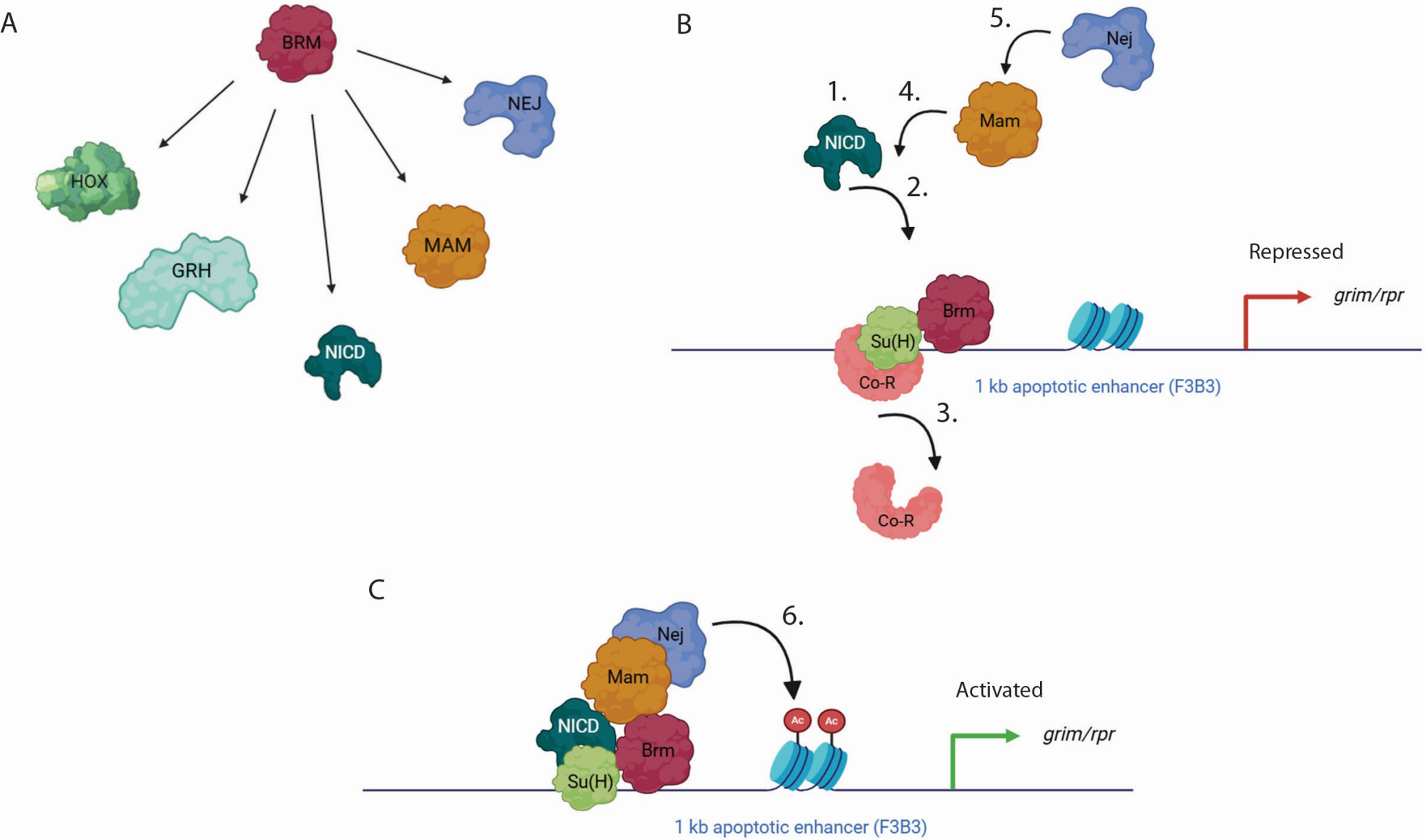
A
BRM
NEJ
HOX
GRH
MAM
NICD
B
5.
Nej
1.
4.
Mam
NICD
2.
Repressed
grim/rpr
Brm
Su(H)
Co-R
1 kb apoptotic enhancer (F3B3)
3.
Co-R
C
6.
Nej
Mam
NICD
Brm
Su(H)
Ac
Ac
Activated
grim/rpr
1 kb apoptotic enhancer (F3B3)

Figure S1

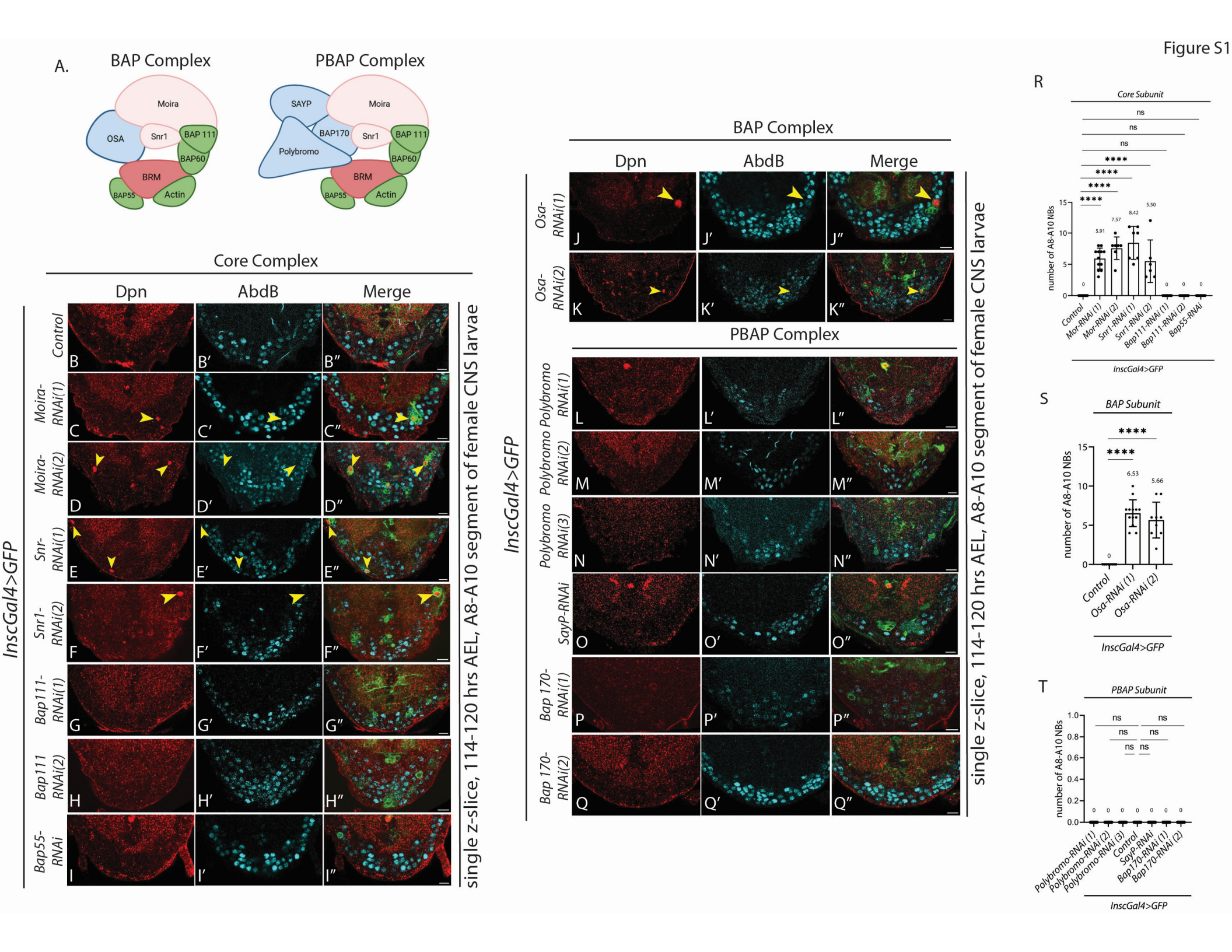
A.
BAP Complex
PBAP Complex
Moira
OSA
Snr1
BAP 111
BAP60
BRM
BAP55
Actin
SAYP
BAP170
Polybromo
Core Complex
Dpn
AbdB
Merge
Control
Moira-RNAi(1)
Moira-RNAi(2)
Snr-RNAi(1)
Snr1-RNAi(2)
Bap111-RNAi(1)
Bap111 RNAi(2)
Bap55-RNAi
InscGal4>GFP
single z-slice, 114-120 hrs AEL, A8-A10 segment of female CNS larvae
Osa-RNAi(1)
Osa-RNAi(2)
Polybromo RNAi(1)
Polybromo RNAi(2)
Polybromo RNAi(3)
SayP-RNAi
Bap 170-RNAi(1)
Bap 170-RNAi(2)
R
Core Subunit
number of A8-A10 NBs
Control
Mor-RNAi (1)
Mor-RNAi (2)
Snr1-RNAi (1)
Snr1-RNAi (2)
Bap111-RNAi (1)
Bap111-RNAi (2)
Bap55-RNAi
S
BAP Subunit
Osa-RNAi (1)
Osa-RNAi (2)
T
PBAP Subunit
Polybromo-RNAi (1)
Polybromo-RNAi (2)
Polybromo-RNAi (3)
SayP-RNAi
Bap170-RNAi (1)
Bap170-RNAi (2)

Figure S2

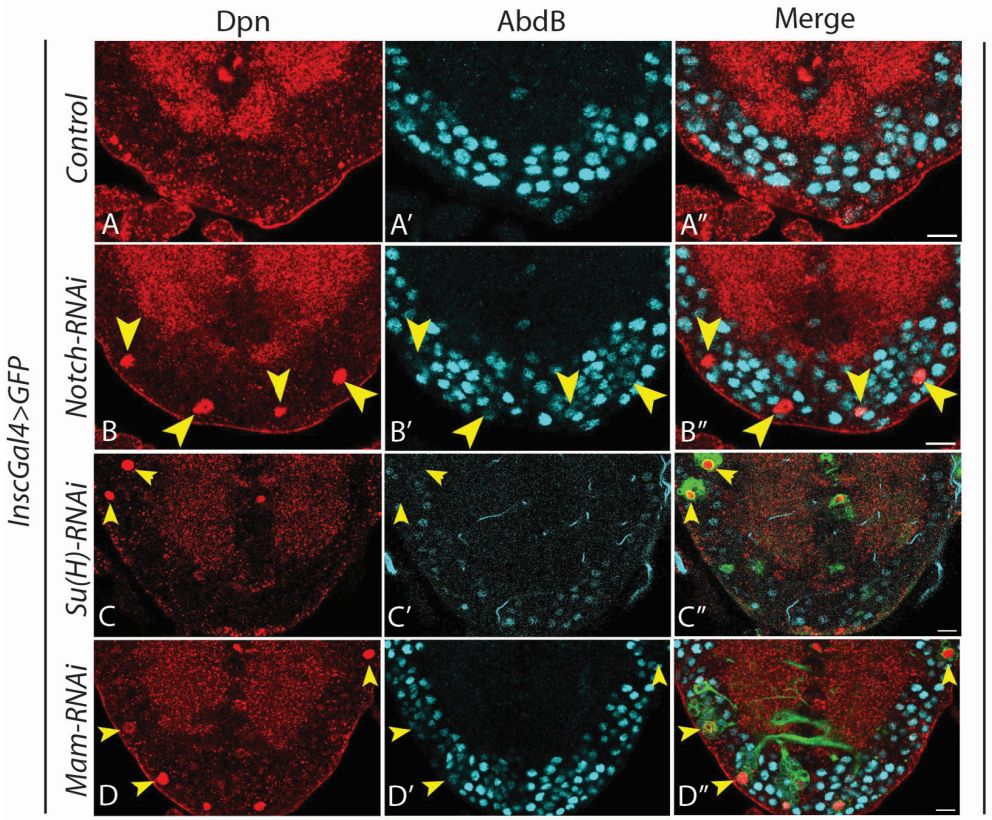
Dpn
AbdB
Merge
InscGal4>GFP
Control
Notch-RNAi
Su(H)-RNAi
Mam-RNAi
A
A′
A″
B
B′
B″
C
C′
C″
D
D′
D″
single z-slice, 114-120 hrs AEL,
A8-A10 segments of female larval CNS

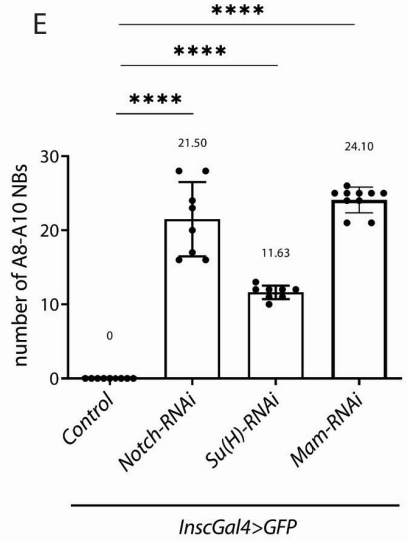
E
****
****
****
number of A8-A10 NBs
30
20
10
0
0
21.50
11.63
24.10
Control
Notch-RNAi
Su(H)-RNAi
Mam-RNAi
InscGal4>GFP

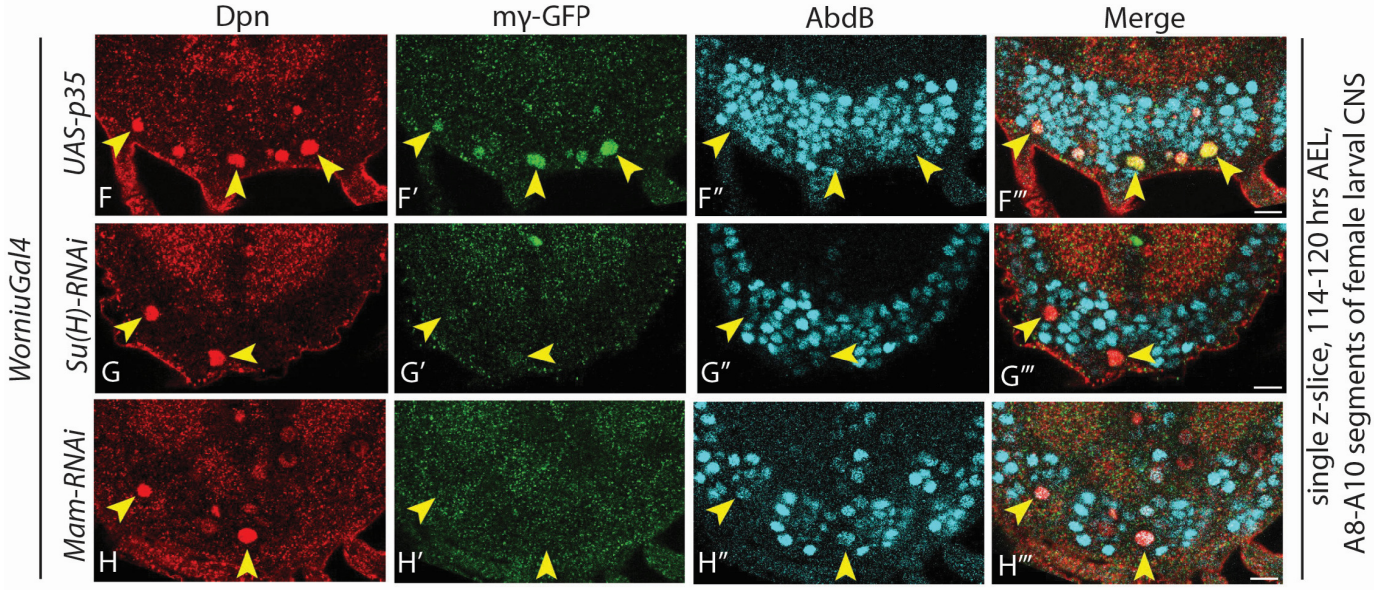
Dpn
mγ-GFP
AbdB
Merge
WorniuGal4
UAS-p35
Su(H)-RNAi
Mam-RNAi
F
F′
F″
F‴
G
G′
G″
G‴
H
H′
H″
H‴
single z-slice, 114-120 hrs AEL,
A8-A10 segments of female larval CNS

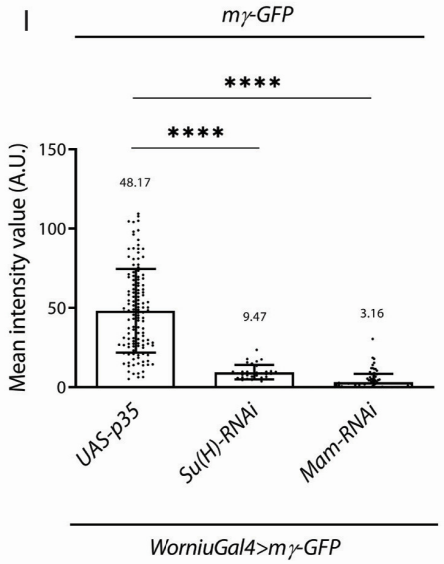
I
mγ-GFP
****
****
Mean intensity value (A.U.)
150
100
50
0
48.17
9.47
3.16
UAS-p35
Su(H)-RNAi
Mam-RNAi
WorniuGal4>mγ-GFP

Figure S3

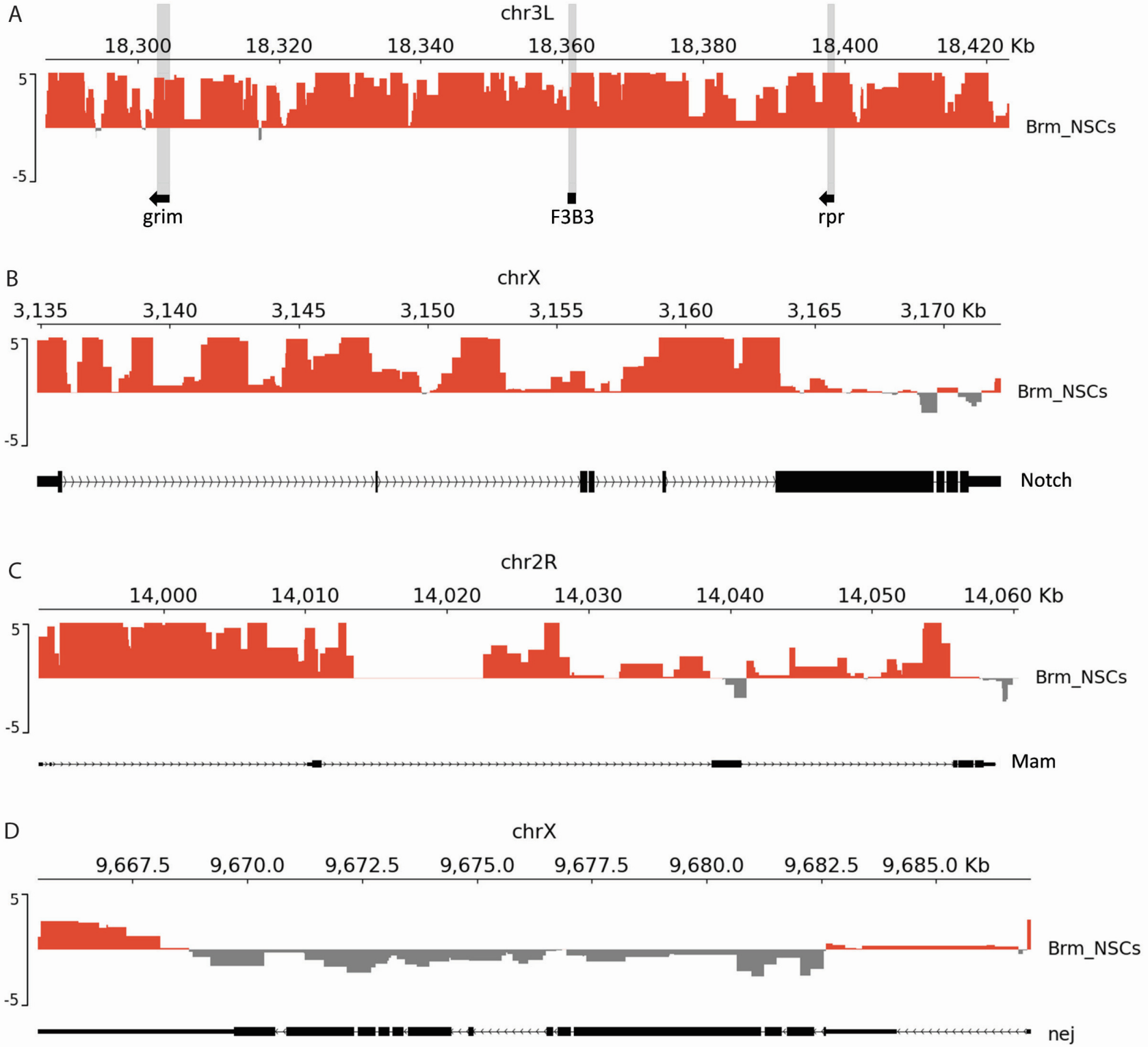
A
chr3L
18,300
18,320
18,340
18,360
18,380
18,400
18,420 Kb
5
-5
Brm_NSCs
grim
F3B3
rpr
B
chrX
3,135
3,140
3,145
3,150
3,155
3,160
3,165
3,170 Kb
5
-5
Brm_NSCs
Notch
C
chr2R
14,000
14,010
14,020
14,030
14,040
14,050
14,060 Kb
5
-5
Brm_NSCs
Mam
D
chrX
9,667.5
9,670.0
9,672.5
9,675.0
9,677.5
9,680.0
9,682.5
9,685.0 Kb
5
-5
Brm_NSCs
nej

RNAi experiments:

A. Embryonic knockdown

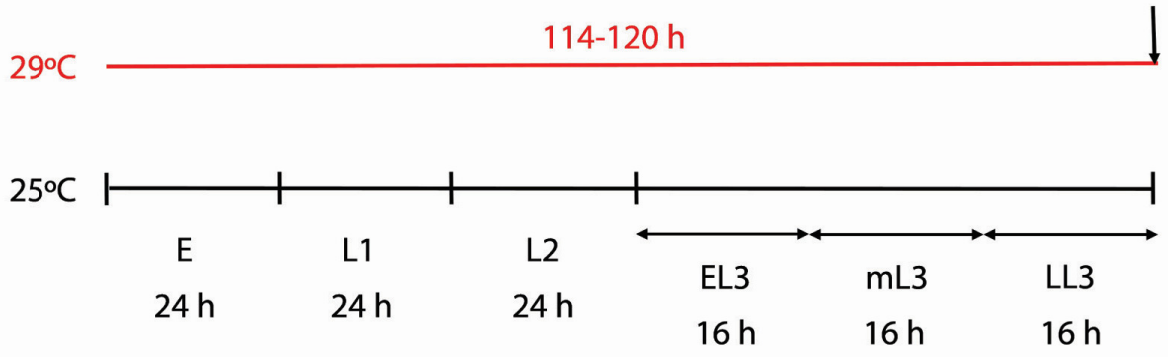

F3B3-LacZ/UAS-p35 experiment:

B. early L1 temperature shift and Late L3 dissection

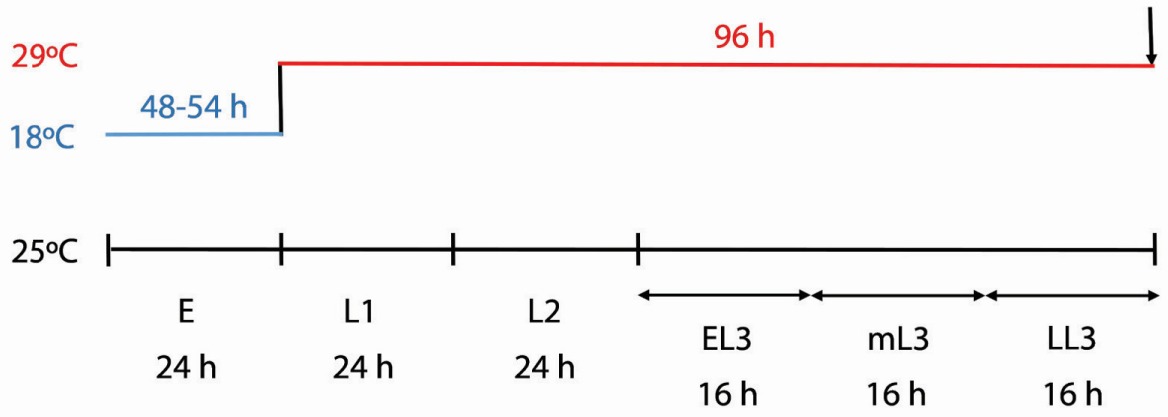

Dam-ID temperature shift experiment:

C. mid L2 temperature shift and mid L3 dissection

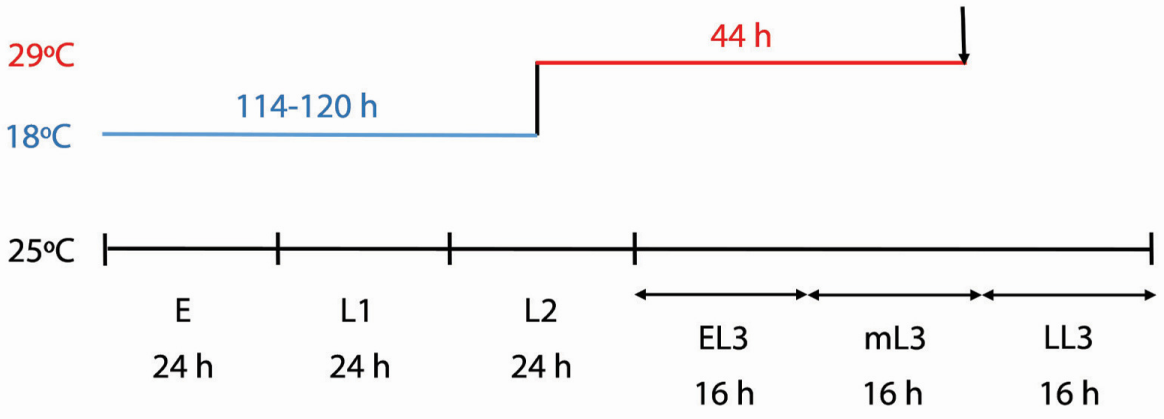

Figure S5

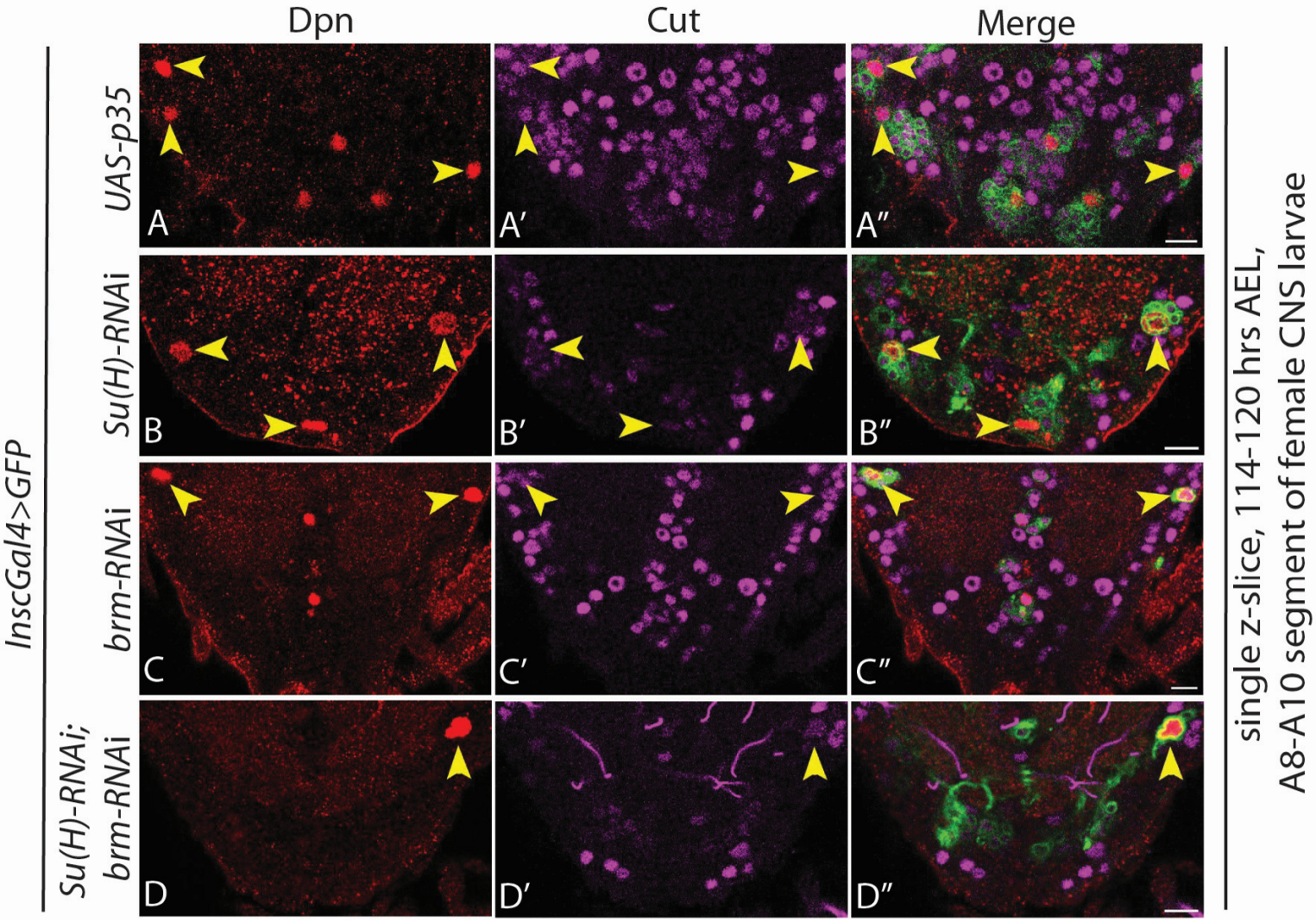
Dpn
Cut
Merge
InscGal4>GFP
UAS-p35
Su(H)-RNAi
brm-RNAi
Su(H)-RNAi; brm-RNAi
A
A′
A″
B
B′
B″
C
C′
C″
D
D′
D″
single z-slice, 114-120 hrs AEL,
A8-A10 segment of female CNS larvae

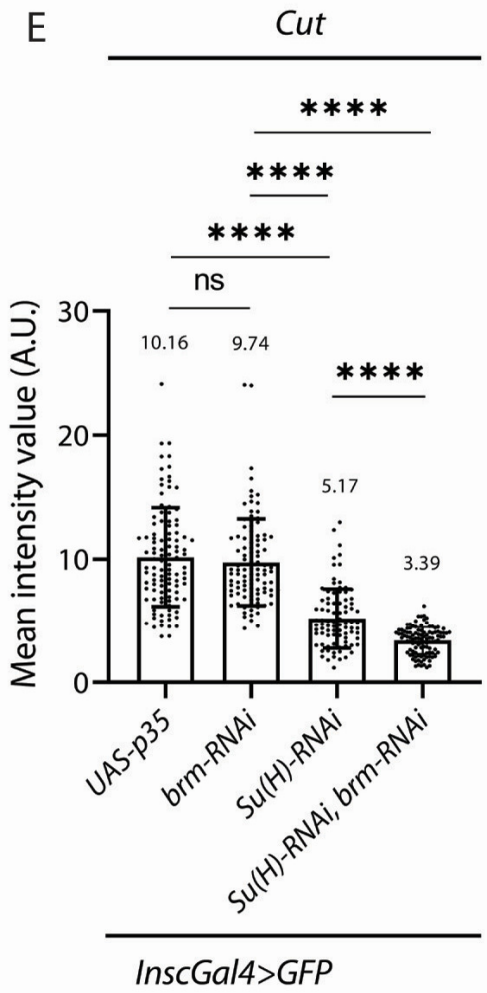
E
Cut
****
****
****
ns
****
Mean intensity value (A.U.)
30
20
10
0
10.16
9.74
5.17
3.39
UAS-p35
brm-RNAi
Su(H)-RNAi
Su(H)-RNAi, brm-RNAi
InscGal4>GFP